

# Star-Shaped Denoising Diffusion Probabilistic Models

Andrey Okhotin <sup>\*1</sup> Dmitry Molchanov <sup>\*1</sup> Vladimir Arkhipkin <sup>2</sup> Grigory Bartosh <sup>3</sup> Aibek Alanov <sup>1,4</sup>  
Dmitry Vetrov <sup>1,4</sup>

## Abstract

Methods based on Denoising Diffusion Probabilistic Models (DDPM) became a ubiquitous tool in generative modeling. However, they are mostly limited to Gaussian and discrete diffusion processes. We propose Star-Shaped Denoising Diffusion Probabilistic Models (SS-DDPM), a model with a non-Markovian diffusion-like noising process. In the case of Gaussian distributions, this model is equivalent to Markovian DDPMs. However, it can be defined and applied with arbitrary noising distributions, and admits efficient training and sampling algorithms for a wide range of distributions that lie in the exponential family. We provide a simple recipe for designing diffusion-like models with distributions like Beta, von Mises–Fisher, Dirichlet, Wishart and others, which can be especially useful when data lies on a constrained manifold such as the unit sphere, the space of positive semi-definite matrices, the probabilistic simplex, etc. We evaluate the model in different settings and find it competitive even on image data, where Beta SS-DDPM achieves results comparable to a Gaussian DDPM.

## 1. Introduction

Deep generative models have shown outstanding sample quality in a wide variety of modalities. Generative Adversarial Networks (GANs) (Goodfellow et al., 2014; Karras et al., 2021), Autoregressive models (Ramesh et al., 2021), Variational Autoencoders (Kingma & Welling, 2013; Rezende et al., 2014), Normalizing Flows (Grathwohl et al., 2018;

<sup>\*</sup>Equal contribution <sup>1</sup>HSE University, Moscow, Russia  
<sup>2</sup>Sber AI, Moscow, Russia <sup>3</sup>MLab, Informatics Institute, University of Amsterdam, Amsterdam, Netherlands  
<sup>4</sup>AIRI, Moscow, Russia. Correspondence to: Andrey Okhotin <[andrey.okhotin@gmail.com](mailto:andrey.okhotin@gmail.com)>, Dmitry Molchanov <[dmolch111@gmail.com](mailto:dmolch111@gmail.com)>, Vladimir Arkhipkin <[arkhipkin.v98@gmail.com](mailto:arkhipkin.v98@gmail.com)>, Grigory Bartosh <[g.bartosh@uva.nl](mailto:g.bartosh@uva.nl)>, Aibek Alanov <[alanov.aibek@gmail.com](mailto:alanov.aibek@gmail.com)>, Dmitry Vetrov <[vetrovd@yandex.ru](mailto:vetrovd@yandex.ru)>.

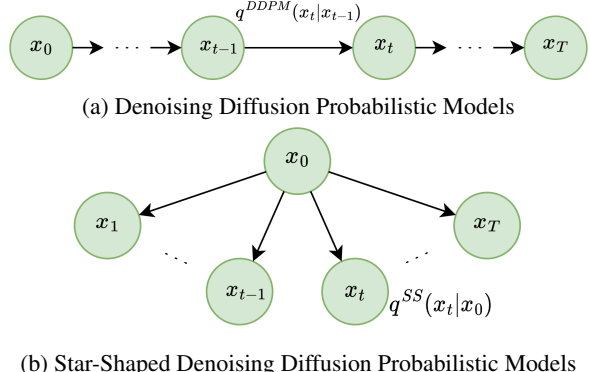


Figure 1: Forward processes of DDPM and SS-DDPM.

Chen et al., 2019) and Energy-based models (Xiao et al., 2020) show impressive abilities to synthesize objects. However, GANs are not robust to the choice of architecture and optimization method (Arjovsky et al., 2017; Gulrajani et al., 2017; Karras et al., 2019; Brock et al., 2018), and they often fail to cover modes in data distribution (Zhao et al., 2018; Thanh-Tung & Tran, 2020). Likelihood-based models do not suffer from collapse modes, but may overestimate the probability in low-density regions (Zhang et al., 2021).

Recently, diffusion probabilistic models (Sohl-Dickstein et al., 2015; Ho et al., 2020) have received attention. These models generate samples using a trained Markov process that starts with white noise and iteratively removes noise from the sample. Recent works have shown that diffusion models can generate samples comparable in quality or even better than GANs (Song et al., 2020b; Dhariwal & Nichol, 2021), while they do not suffer from mode collapse by design, and also they have a log-likelihood comparable to Autoregressive models (Kingma et al., 2021). Moreover, diffusion models show these results in various modalities such as images (Saharia et al., 2021), sound (Popov et al., 2021; Liu et al., 2022) and shapes (Luo & Hu, 2021; Zhou et al., 2021).

The main principle of diffusion models is to destroy information during the forward process and then restore it during the reverse process. In conventional diffusion models like denoising diffusion probabilistic model (DDPM)

destruction of information occurs through the injection of Gaussian noise, which is reasonable for some types of data, such as images. However, for data distributed on manifolds, bounded volumes, or with other features, the injection of Gaussian noise can be unnatural, breaking the data structure. For such data, one might want to use non-Gaussian noise that takes the data structure into account.

Unfortunately, it is not clear how to replace the noise distribution within traditional diffusion models. The problem is that we have to maintain a connection between the distributions defining the Markov noising process that gradually destroys information and its marginal distributions. While some papers explore other distributions, such as delta functions (Bansal et al., 2022) or Gamma distribution (Nachmani et al., 2021), they provide ad hoc solutions for special cases that are not easily generalized.

In this paper, we present Star-Shaped Denoising Diffusion Probabilistic Models (SS-DDPM), a new approach that generalizes Gaussian DDPM to an exponential family of noise distributions. In SS-DDPM, one only needs to define marginal distributions at each diffusion step (see Figure 1). We provide a derivation of SS-DDPM, design an efficient sampling and training algorithms, and show its equivalence to DDPM (Ho et al., 2020) in the case of Gaussian noise. Then, we outline a number of practical considerations that aid in training and applying SS-DDPMs. In Section 4, we demonstrate the ability of SS-DDPM to work with distributions like von Mises–Fisher, Dirichlet and Wishart. Finally, we define and train a Beta diffusion model on CIFAR-10, achieving results, comparable to a Gaussian DDPM.

## 2. Theory

We start by briefly reminding the definition of DDPM (Ho et al., 2020) and describing its limitations. We then introduce SS-DDPM by challenging one of the main design principles behind DDPMs.

### 2.1. DDPMs

The Gaussian DDPM (Ho et al., 2020) is defined as a forward (diffusion) process  $q^{\text{DDPM}}(x_{0:T})$  and a corresponding reverse (denoising) process  $p_{\theta}^{\text{DDPM}}(x_{0:T})$ . The forward process is defined as a Markov chain with Gaussian conditionals:

$$q^{\text{DDPM}}(x_{0:T}) = q(x_0) \prod_{t=1}^T q^{\text{DDPM}}(x_t | x_{t-1}) \quad (1)$$

$$q^{\text{DDPM}}(x_t | x_{t-1}) = \mathcal{N}(x_t; \sqrt{1 - \beta_t} x_{t-1}, \beta_t \mathbf{I}) \quad (2)$$

where  $q(x_0)$  is the data distribution. Parameters  $\beta_t$  are typically chosen in advance and fixed, defining the noise schedule of the diffusion process. The noise schedule

is chosen in such a way that the final  $x_T$  no longer depends on  $x_0$  and follows a standard Gaussian distribution  $q^{\text{DDPM}}(x_T) = \mathcal{N}(x_T; 0, \mathbf{I})$ .

The reverse process  $p_{\theta}^{\text{DDPM}}(x_{0:T})$  follows a similar structure and constitutes a generative part of the model:

$$p_{\theta}^{\text{DDPM}}(x_{0:T}) = q^{\text{DDPM}}(x_T) \prod_{t=1}^T p_{\theta}^{\text{DDPM}}(x_{t-1} | x_t) \quad (3)$$

$$p_{\theta}^{\text{DDPM}}(x_{t-1} | x_t) = \mathcal{N}(x_{t-1}; \mu_{\theta}(x_t, t), \Sigma_{\theta}(x_t, t)) \quad (4)$$

The forward process  $q^{\text{DDPM}}(x_{0:T})$  of DDPM is typically fixed, and all the parameters of the model are contained in the generative part of the model  $p_{\theta}^{\text{DDPM}}(x_{0:T})$ . These parameters are tuned to maximize the variational lower bound (VLB) on the likelihood of the training data:

$$\mathcal{L}^{\text{DDPM}}(\theta) = \mathbb{E}_{q^{\text{DDPM}}} \left[ \log p_{\theta}^{\text{DDPM}}(x_0 | x_1) - \right] \quad (5)$$

$$- \sum_{t=2}^T D_{KL}(q^{\text{DDPM}}(x_{t-1} | x_t, x_0) \| p_{\theta}^{\text{DDPM}}(x_{t-1} | x_t)) \quad (6)$$

$$\mathcal{L}^{\text{DDPM}}(\theta) \rightarrow \max_{\theta} \quad (7)$$

DDPM can also be defined for categorical (Hoogeboom et al., 2021) and Gamma (Nachmani et al., 2021) distributions.

### 2.2. Limitation of DDPMs

Suppose we are tasked with constructing a generative model for data that is distributed on some manifold, e.g. on a unit sphere. While it may be tempting to consider utilizing a conventional DDPM, such a model would treat our data as points in Euclidean space and thereby noisy objects would no longer lie on a unit sphere. Consequently, the generative model would expend a significant portion of its resources to learn what is already known from the specifics of the given problem—that the real-world data resides on a sphere.

A more efficient way would be to inject a noise such that the noisy objects remain on the same sphere. Then the model will not waste its limited resources in learning the manifold, and generate objects lying on it by design. One possible method of generating such noise is through the von Mises–Fisher distribution. In order to construct a DDPM, we must define the transition between two neighboring steps of diffusion,  $x_{t-1}$  and  $x_t$ . For instance, we could sample from the von Mises–Fisher distribution,  $q(x_t | x_{t-1})$ , with a mode of  $x_{t-1}$  and some large concentration parameter  $\kappa$ .

However, a problem arises when attempting to complete the DDPM, as we also require the explicit form of the marginals,  $q(x_t | x_0)$ . This is needed for computation of  $q(x_{t-1} | x_t, x_0)$  that is a key ingredient in equation (6). Those marginals can

be computed for Gaussian or Gamma noise due to the fact that these distributions are a conjugate prior to itself, and for categorical distributions in the case of discrete data. In general, however, we cannot know both the transition and marginal distributions in explicit form, which is a crucial requirement for constructing a DDPM. As such, the conventional DDPM framework is currently unable to process the injection of noise other than Gaussian, Gamma or categorical. To overcome this limitation, we must alter the way we build the diffusion model by bypassing the explicit definition of the transition distribution,  $q(x_t|x_{t-1})$ , and starting from the marginal distribution,  $q(x_t|x_0)$ , instead.

### 2.3. Star-Shaped DDPMs

As previously discussed, extending the DDPM model to other distributions poses significant challenges. Specifically, we must define the steps,  $q(x_t|x_{t-1})$ , in a manner that enables us to compute the explicit form of the marginals,  $q(x_t|x_0)$ , and also compute the posterior distributions,  $q(x_{t-1}|x_t, x_0)$ , which is only feasible for simple distributions such as Gaussian, Gamma (Nachmani et al., 2021), and categorical (Hoogeboom et al., 2021).

In light of these difficulties, we propose to construct a model that only relies on marginal distributions,  $q(x_t|x_0)$ , in its definition and the derivation of the loss function.

We define a star-shaped diffusion with the *non-Markovian* forward process  $q^{\text{ss}}(x_{0:T})$  that has the following structure:

$$q^{\text{ss}}(x_{0:T}) = q(x_0) \prod_{t=1}^T q^{\text{ss}}(x_t|x_0), \quad (8)$$

where  $q(x_0)$  is the data distribution. We note that in contrast to DDPM all noisy variables  $x_t$  are conditionally independent given  $x_0$  instead of constituting a Markov chain. This structure of the forward process allows us to utilize other noise distributions, which we discuss in more detail later.

### 2.4. Defining the reverse model

In DDPMs the true reverse model  $q^{\text{DDPM}}(x_{0:T})$  has a Markovian structure (Ho et al., 2020), allowing for an efficient sequential generation algorithm:

$$q^{\text{DDPM}}(x_{0:T}) = q^{\text{DDPM}}(x_T) \prod_{t=1}^T q^{\text{DDPM}}(x_{t-1}|x_t). \quad (9)$$

For a star-shaped diffusion, however, the Markovian assumption breaks:

$$q^{\text{ss}}(x_{0:T}) = q^{\text{ss}}(x_T) \prod_{t=1}^T q^{\text{ss}}(x_{t-1}|x_{t:T}) \quad (10)$$

Consequently we now need to approximate the true reverse process by a parametric model which is conditioned on the

whole tail  $x_{t:T}$ .

$$p_{\theta}^{\text{ss}}(x_{0:T}) = p_{\theta}^{\text{ss}}(x_T) \prod_{t=1}^T p_{\theta}^{\text{ss}}(x_{t-1}|x_{t:T}) \quad (11)$$

It is important to use the whole tail  $x_{t:T}$  rather than just  $x_t$  when predicting  $x_{t-1}$  in star-shaped model. As we show in Appendix B, if we try to approximate the true reverse process with a Markov model, we introduce a substantial irreducible gap into the variational lower bound. More crucially, such sampling procedure fails to generate realistic samples, as can be seen in Figure 3. Intuitively, in DDPMs the information about  $x_0$  that is contained in  $x_{t+1}$  is nested into the information about  $x_0$  that is contained in  $x_t$ . That is why knowing  $x_t$  allows us to discard  $x_{t+1}$ . In star-shaped diffusion, however, all variables contain independent pieces of information about  $x_0$  and should all be taken into account when making predictions. A similar effect was observed in Cold Diffusion (Bansal et al., 2022), which also required a modified sampling scheme.

We can write down the variational lower bound as follows (see Appendix A for details):

$$\begin{aligned} \mathcal{L}^{\text{ss}}(\theta) = \mathbb{E}_{q^{\text{ss}}} \left[ \log p_{\theta}(x_0|x_{1:T}) - \right. \\ \left. - \sum_{t=2}^T D_{KL}(q^{\text{ss}}(x_{t-1}|x_0) \| p_{\theta}^{\text{ss}}(x_{t-1}|x_{t:T})) \right] \end{aligned} \quad (12)$$

With this VLB we only need the marginal distributions  $q(x_{t-1}|x_0)$  to define and train the model, which allows us to use a wider variety of noising distributions. Since conditioning the predictive model  $p_{\theta}(x_{t-1}|x_{t:T})$  on the whole tail  $x_{t:T}$  is typically not practical, we propose a more efficient way to implement the reverse process next.

### 2.5. Efficient tail conditioning

Instead of using the full tail  $x_{t:T}$ , we would like to define a variable  $G_t = \mathcal{G}_t(x_{t:T})$  that would extract all information about  $x_0$  from the tail  $x_{t:T}$ . Formally speaking, we would like for the following equality to hold:

$$q^{\text{ss}}(x_{t-1}|x_{t:T}) = q^{\text{ss}}(x_{t-1}|G_t) \quad (13)$$

One way to define  $G_t$  is to concatenate all the variables  $x_{t:T}$  into a single vector. This, however, is impractical, as its dimension would grow with the size of the tail  $T - t + 1$ .

The role of  $G_t$  is that of a sufficient statistic for the tail  $x_{t:T}$ . The Pitman–Koopman–Darroch (Pitman, 1936) theorem (PKD) states that exponential families admit a sufficient statistic with constant dimensionality. It also states that no other distribution admits one: if such statistic were to exist, the distribution has to be a member of the exponential family.

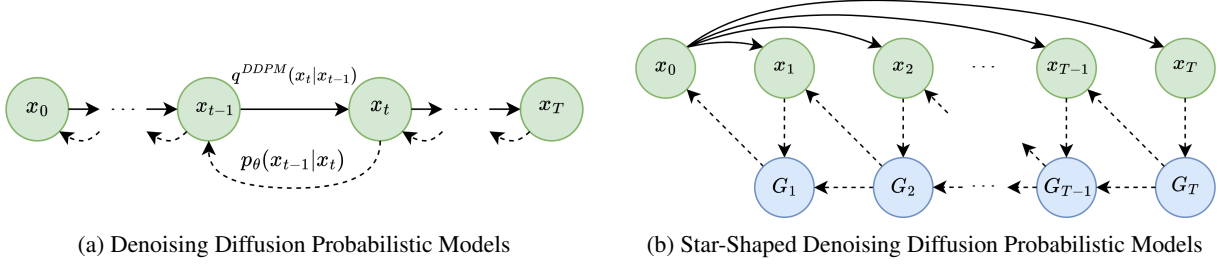


Figure 2: Model structure of DDPM and SS-DDPM.

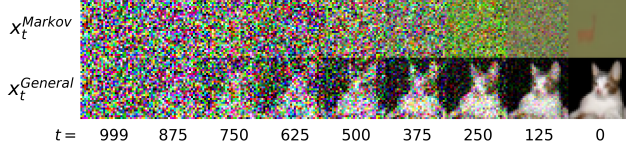


Figure 3: Markov reverse process fails to recover realistic images from star-shaped diffusion, while a general reverse process produces realistic images.

Inspired by the PKD, we turn to the exponential family of distributions. In the case of star-shaped diffusion, we cannot apply the PKD directly, as it was formulated for i.i.d. samples and our samples are not identically distributed. However, we can still define a *sufficient tail statistic*  $G_t$  for a specific subset of exponential family, which we call an *exponential family with linear parameterization*:

**Theorem 1.** *Given*

$$q^{\text{ss}}(x_t|x_0) = h_t(x_t) \exp \{ \eta_t(x_0)^\top \mathcal{T}(x_t) - \Omega_t(x_0) \} \quad (14)$$

$$\eta_t(x_0) = A_t f(x_0) + b_t \quad (15)$$

$$G_t = \mathcal{G}_t(x_{t:T}) = \sum_{s=t}^T A_s^\top \mathcal{T}(x_s) \quad (16)$$

the following holds:

$$q^{\text{ss}}(x_{t-1}|x_{t:T}) = q^{\text{ss}}(x_{t-1}|G_t) \quad (17)$$

We prove this equality in Appendix C. When  $A_t$  is scalar, we denote it as  $a_t$  instead.

For the most part, the premise of Theorem 1 restricts the parameterization of the distributions rather than the family of the distributions involved. As we discuss in Appendix E, we found it easy to come up with linear parameterization for a wide range of distributions in the exponential family. For example, we can obtain a linear parameterization for the Beta distribution  $q(x_t|x_0) = \text{Beta}(x_t; \alpha_t, \beta_t)$  using  $x_0$  as the mode of the distribution and introducing a new concentration parameter  $\nu_t$ :

$$\alpha_t = 1 + \nu_t x_0 \quad (18)$$

$$\beta_t = 1 + \nu_t (1 - x_0) \quad (19)$$

In this case  $\eta_t(x_0) = \nu_t x_0$ ,  $\mathcal{T}(x_t) = \log \frac{x_t}{1-x_t}$ , and we can use (16) to define the tail statistic  $G_t$ . We provide more examples in Appendix E and summarize these results in Table 2.

We suspect that, just like in PKD, this trick is only possible for a subset of exponential family. In general case the dimensionality of  $G_t$  would grow with the size of the tail  $x_{t:T}$ . It is still possible to apply SS-DDPM in this case, however, crafting the (now only approximately) sufficient statistic  $G_t$  would require a more careful consideration and we leave it for future work.

## 2.6. Final model definition

To maximize the VLB (12), each step of the reverse process should approximate the true reverse distribution:

$$\begin{aligned} p_\theta^{\text{ss}}(x_{t-1}|x_{t:T}) &\approx q^{\text{ss}}(x_{t-1}|x_{t:T}) = \\ &= \int q^{\text{ss}}(x_{t-1}|x_0) q^{\text{ss}}(x_0|x_{t:T}) dx_0 \end{aligned} \quad (20)$$

Similar to DDPM (Ho et al., 2020), we choose to approximate  $q^{\text{ss}}(x_0|x_{t:T})$  with a delta function centered at the prediction of some model  $x_\theta(\mathcal{G}_t(x_{t:T}), t)$ . This results in the following definition of the reverse process of SS-DDPM:

$$p_\theta^{\text{ss}}(x_{t-1}|x_{t:T}) = q^{\text{ss}}(x_{t-1}|x_0)|_{x_0=x_\theta(\mathcal{G}_t(x_{t:T}), t)} \quad (21)$$

The distribution  $p_\theta^{\text{ss}}(x_0|x_{1:T})$  can be fixed to some small-variance distribution  $p^{\text{ss}}(x_0|x_1)$  centered at  $x_1$ , similar to the dequantization term, commonly used in DDPM.

Together with the forward process (8) and the VLB objective (12), this concludes the general definition of the SS-DDPM model. The model structure is illustrated in Figure 2. The corresponding training and sampling algorithms are provided in Algorithms 1 and 2.

The resulting model is similar to DDPM in spirit. We follow the same principles when designing the forward process: starting from a low-variance distribution, centered at  $x_0$  at  $t=1$ , we gradually increase the entropy of the distribution

**Algorithm 1** SS-DDPM training

---

```

repeat
     $x_0 \sim q(x_0)$ 
     $t \sim \text{Uniform}(1, \dots, T)$ 
     $x_{t:T} \sim q^{\text{ss}}(x_{t:T}|x_0)$ 
     $G_t = \sum_{s=t}^T A_s^T \mathcal{T}(x_s)$ 
    Move along  $\nabla_{\theta} \text{KL}(q^{\text{ss}}(x_{t-1}|x_0) \| p_{\theta}^{\text{ss}}(x_{t-1}|G_t))$ 
until Convergence

```

---

**Algorithm 2** SS-DDPM sampling

---

```

 $x_T \sim q^{\text{ss}}(x_T)$ 
 $G_T = A_T^T \mathcal{T}(x_T)$ 
for  $t = T$  to 2 do
     $\tilde{x}_0 = x_{\theta}(G_t, t)$ 
     $x_{t-1} \sim q^{\text{ss}}(x_{t-1}|x_0) |_{x_0=\tilde{x}_0}$ 
     $G_{t-1} = G_t + A_{t-1}^T \mathcal{T}(x_{t-1})$ 
end for
 $x_0 \sim p_{\theta}^{\text{ss}}(x_0|G_1)$ 

```

---

$q^{\text{ss}}(x_t|x_0)$  until there is no information shared between  $x_0$  and  $x_t$  at  $t = T$ .

We provide concrete definitions for Beta, Gamma, Dirichlet, von Mises, von Mises–Fisher, Wishart, Gaussian and Categorical distributions in Appendix E. We also present these results in form of a cheat-sheet in Table 2.

## 2.7. Connection to DDPMs

The tail statistics  $G_t$  form a diffusion-like Markov process that can be seen as dual to the star-shaped process on  $x_t$ . Interestingly, in Gaussian SS-DDPM this dual process is itself a Gaussian DDPM with a particular noising schedule:

**Theorem 2.** Let  $\bar{\alpha}_t^{\text{DDPM}}$  define the noising schedule for a DDPM model (1–2) via  $\beta_t = (\bar{\alpha}_{t-1}^{\text{DDPM}} - \bar{\alpha}_t^{\text{DDPM}})/\bar{\alpha}_{t-1}^{\text{DDPM}}$ . Let  $q^{\text{ss}}(x_{0:T})$  be a Gaussian SS-DDPM forward process with the following noising schedule and tail statistic:

$$q^{\text{ss}}(x_t|x_0) = \mathcal{N}\left(x_t; \sqrt{\bar{\alpha}_t^{\text{ss}}} x_0, 1 - \bar{\alpha}_t^{\text{ss}}\right), \quad (22)$$

$$G_t(x_{t:T}) = \frac{1 - \bar{\alpha}_t^{\text{DDPM}}}{\sqrt{\bar{\alpha}_t^{\text{DDPM}}}} \sum_{s=t}^T \frac{\sqrt{\bar{\alpha}_s^{\text{ss}}} x_s}{1 - \bar{\alpha}_s^{\text{ss}}}, \text{ where} \quad (23)$$

$$\frac{\bar{\alpha}_t^{\text{ss}}}{1 - \bar{\alpha}_t^{\text{ss}}} = \frac{\bar{\alpha}_t^{\text{DDPM}}}{1 - \bar{\alpha}_t^{\text{DDPM}}} - \frac{\bar{\alpha}_{t+1}^{\text{DDPM}}}{1 - \bar{\alpha}_{t+1}^{\text{DDPM}}}. \quad (24)$$

Then the tail statistic  $G_t$  follows a Gaussian DDPM noising process  $q^{\text{DDPM}}(x_{0:T})|_{x_{1:T}=G_{1:T}}$  defined by the schedule  $\bar{\alpha}_t^{\text{DDPM}}$ . Moreover, the corresponding reverse processes and VLB objectives are also equivalent.

We show this equivalence in Appendix D. Since the Gaussian SS-DDPM is equivalent to a Gaussian DDPM, the SS-DDPM can be seen as a direct generalization of the DDPM

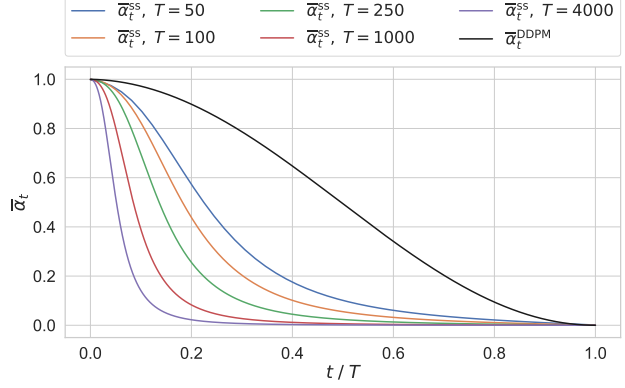


Figure 4: The noising schedule  $\bar{\alpha}_t^{\text{ss}}$  for Gaussian star-shaped diffusion, defined for different numbers of steps  $T$  using (24). All the corresponding equivalent DDPMs have the same cosine schedule  $\bar{\alpha}_t^{\text{DDPM}}$ .

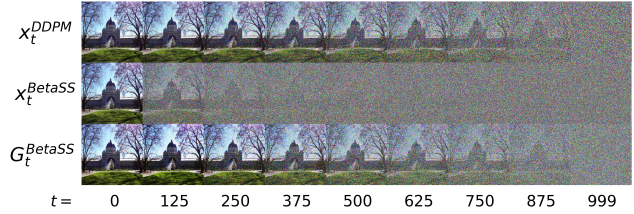


Figure 5: Top: samples  $x_t$  from a Gaussian DDPM forward process with a cosine noise schedule. Bottom: samples  $G_t$  from a Beta SS-DDPM forward process with a noise schedule, obtained by matching the mutual information as described in Appendix F. Middle: corresponding samples  $x_t$  from that Beta SS-DDPM forward process. The tail statistics have the same level of noise as  $x_t^{\text{DDPM}}$ , while the samples  $x_t^{\text{BetaSS}}$  are diffused much faster.

model. We make use of this connection when choosing the noising schedule for other distributions, as discussed in Appendix F.

In the general case, the explicit description of Markov diffusion process for  $G_t$  is problematic and it is easier to work directly with star-shaped model for  $x_t$ . We leave the derivation of general description of diffusion process for  $G_t$  for future research.

## 3. Practical considerations

While the model is properly defined, there are several practical considerations that are important for the efficiency of star-shaped diffusion.

**Choosing the right schedule** It is important to choose the right noising schedule for a SS-DDPM model. It significantly depends on the number of diffusion steps  $T$ , and

behaves differently given different noising schedules, typical to DDPMs. This is illustrated in Figure 4, where we show the noising schedules for Gaussian SS-DDPMs that are equivalent to DDPMs with the same cosine schedule.

Since the variables  $G_t$  follow a DDPM-like process, we would like to somehow reuse those DDPM noising schedules that are already known to work well. For Gaussian distributions we can transform a DDPM noising schedule into the corresponding SS-DDPM noising schedule analytically by equating  $I(x_0; G_t) = I(x_0; x_t^{\text{DDPM}})$ . In general case we look for schedules that have approximately the same level of mutual information  $I(x_0; G_t)$  as the corresponding mutual information  $I(x_0; x_t^{\text{DDPM}})$  for a DDPM model for all timesteps  $t$ . We estimate the mutual information using Kraskov (Kraskov et al., 2004) and DSIVI (Molchanov et al., 2019) estimators, and build a look-up table to match the noising schedules. This procedure is described in more detail in Appendix F. The resulting schedule for the Beta SS-DDPM is illustrated in Figure 5.

**Implementing the sampler** During sampling, we can grow the tail statistic  $G_t$  without any overhead, as described in Algorithm 2. However, during training we need to sample the tail statistic for each object to estimate the loss function. For this we need to sample the full tail  $x_{t:T}$  from the forward process  $q^{\text{ss}}(x_{t:T}|x_0)$ , and then compute the tail statistic  $G_t$ . In practice this does not add a noticeable overhead, and can be computed in parallel to the training process if needed.

**Reducing the number of steps** We can sample from DDPMs more efficiently by skipping some timestamps. This wouldn't work for SS-DDPM, because changing the number of steps would require to change the noising schedule and, consequently, to retrain the model.

However, we can still use a similar trick to reduce the number of function evaluations. Instead of skipping some timestamps  $x_{t_1+1:t_2-1}$ , we can draw them from the forward process using the current prediction  $x_\theta(G_{t_2}, t_2)$ , and then use these samples to obtain the tail statistic  $G_{t_1}$ . For Gaussian SS-DDPM this is equivalent to skipping these timestamps in the corresponding DDPM. In general case it amounts to approximating the reverse process with a different reverse process:

$$\begin{aligned} p_\theta^{\text{ss}}(x_{t_1:t_2}|G_{t_2}) &= \prod_{t=t_1}^{t_2} q^{\text{ss}}(x_t|x_0)|_{x_0=x_\theta(G_{t_2}, t_2)} \approx \\ &\approx \prod_{t=t_1}^{t_2} q^{\text{ss}}(x_t|x_0)|_{x_0=x_\theta(G_{t_2}, t_2)} \end{aligned} \quad (25)$$

In practice we observe a similar dependence on the number of function evaluations for SS-DDPMs and DDPMs. See Appendix H for more details.

**Time-dependent tail normalization** As defined in Theorem 1, the tail statistics can have vastly different scales for different timestamps. The values of coefficients  $a_t$  can range from thousandths when  $t$  approaches  $T$  to thousands when  $t$  approaches zero. To make the tail statistics suitable for use in neural networks, proper normalization is crucial.

As we show in Figure 14, normalizing the tail statistics by the sum of coefficients  $\sum_{s=t}^T a_s$  is not enough. Instead, we collect the time-dependent means and variances of the tail statistics across the training dataset, and normalize the tail statistics to zero mean and unit variance.

Proper normalization is also crucial for the visualization of the tail statistics. After matching the mean and the variance of the tail statistics to those of the sufficient statistics of the training data  $\mathcal{T}(x_0)$ , we can map the normalized tail statistics  $\tilde{G}_t$  into the data domain using  $\mathcal{T}^{-1}(\tilde{G}_t)$ , and visualize them there. The effects of normalization in this case are illustrated in Figure 15.

**Architectural choices** To make training the model easier, we make some minor adjustments to the neural network architecture and the loss function.

Our neural networks  $x_\theta(G_t, t)$  take the tail statistic  $G_t$  as an input and are expected to produce an estimate of  $x_0$  as an output. In SS-DDPM the data  $x_0$  might lie on some manifold, like the unit sphere or the space of positive definite matrices. Therefore, we need to map the neural network output to that manifold. We do that on a case-by-case basis, as described in the corresponding subsections.

Different terms of the VLB can have drastically different scales. For this reason it is common practice to train DDPMs with a modified loss function like  $L_{\text{simple}}$  rather than the VLB to improve the stability of training (Ho et al., 2020). We follow a similar intuition and optimize a reweighted variational lower bound, as described in Section 4.

## 4. Experiments

First, we apply SS-DDPM to various manifolds by considering the von Mises–Fisher, Dirichlet and Wishart diffusion processes. We train and sample from the Dirichlet and Wishart SS-DDPM using  $T = 64$  steps, and use  $T = 100$  steps for the von Mises–Fisher SS-DDPM. We use a MLP with 3 hidden layers of size 512, swish activations and residual connections through hidden layers (He et al., 2015). We use sinusoidal positional time embeddings (Vaswani et al., 2017) of size 32 and concatenate them with the normalized tail statistics  $\tilde{G}_t$ . On top of the network we add a mapping to the corresponding domain. We use noise schedule parameterization described in Table 2 and use time-dependent tail normalization in all experiments with SS-DDPM. The corresponding forward processes are

illustrated in Figures 8, 9 and 10.

The results of these experiments are presented in Table 1. This demonstrates the ability of SS-DDPM to work with different distributions and generate data from exotic domains.

#### 4.1. Geodesic data

We apply SS-DDPM to a geodesic dataset of fires on the Earth surface (EOSDIS, 2020) using a three-dimensional von Mises–Fisher distribution as defined in Table 2. We optimize a simplified loss function, defined as  $\sum_{t=1}^T (1 - x_0^\top x_\theta(G_t, t))$ . To map the prediction to the unit sphere, we normalize the three-dimensional output of the MLP. We train the MLP using the AdamW (Loshchilov & Hutter) optimizer with learning rate of  $2 \times 10^{-4}$  for 500k iterations and batch size 100. We use EMA weights with decay of 0.9999 for inference, and use 100 steps of the reverse process to produce the resulting samples.

#### 4.2. Synthetic data

We evaluate Dirichlet SS-DDPM on a synthetic problem of generating objects on a three-dimensional probabilistic simplex. We use a mixture of three Dirichlet distributions with different parameters as training data. To map the predictions to the domain, we put a `Softmax` function on the top of the MLP. We optimize the VLB without any modifications. We train the MLP using Adam (Kingma & Ba, 2015) with learning rate of  $10^{-4}$  for 60k iterations and batch size 128. We use gradient clipping and EMA weights to improve stability.

We evaluate Wishart SS-DDPM on a synthetic problem of generating symmetric positive definite matrices of size  $2 \times 2$ . We use a mixture of three Wishart distributions with different parameters as training data. For the case of symmetric positive definite matrices  $V$ , MLP predicts a lower triangular factor  $L_\theta$  from the Cholesky decomposition  $V_\theta = L_\theta L_\theta^\top$ . For stability of sampling from the Wishart distribution and estimation of the loss function, we add a scalar matrix  $10^{-4}\mathbf{I}$  to the predicted symmetric positive definite matrix  $V_\theta$ . In Wishart SS-DDPM we use analogue of  $L_{simple}$  as a loss function. To improve the training stability we also divide each KL term corresponding to a timestamp  $t$  by  $n_t$ , the de-facto concentration parameter from the used noising schedule (see Table 2). We train MLP similar to the Dirichlet case and additionally use an exponential learning rate scheduler to mitigate training instabilities. We use a base learning rate of  $10^{-4}$  with an exponential scheduler with  $\gamma = 0.99996$ , batch size 128 and train the MLP for 100k iterations. Since positive definite  $2 \times 2$  matrices can be interpreted as ellipses, we visualize the samples by drawing the corresponding ellipses.

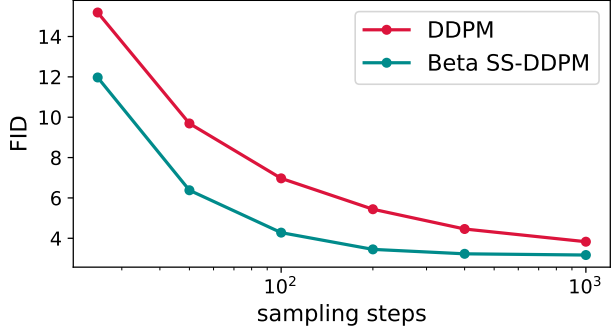


Figure 6: Quality of images, generated using Beta SS-DDPM and DDPM with different numbers of sampling steps, as measured by FID (Fréchet Inception Distance, (Heusel et al., 2017)). Models are trained and evaluated on CIFAR-10. DDPM results taken from (Nichol & Dhariwal, 2021).

#### 4.3. Images

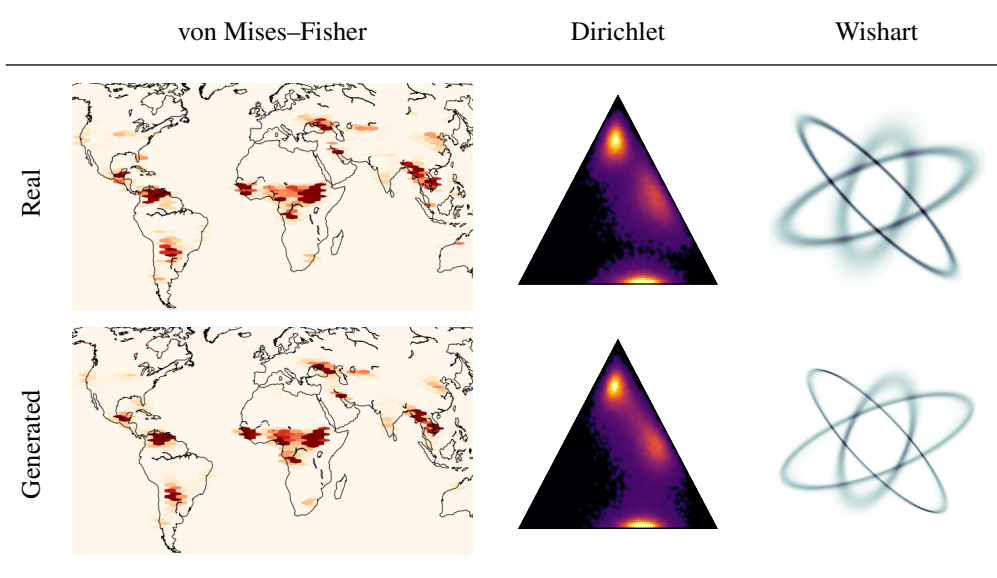
Finally, we evaluate the Beta SS-DDPM on CIFAR-10. Beta diffusion can be applied to images because the training data is typically constrained to a  $[0, 1]$  segment. We use NCSN++ neural network architecture and train strategy from (Song et al., 2020b). We put a sigmoid function on the top of NCSN++ to map the predictions to the data domain. We train Beta SS-DDPM with  $T = 1000$ . We matched the noise schedule in Beta SS-DDPM to the cosine noise schedule in Gaussian DDPM (Nichol & Dhariwal, 2021) in terms of mutual information, as described in Appendix F. Following Improved DDPM (Nichol & Dhariwal, 2021), we evaluate our model with various numbers of generation steps, as described in Appendix H, and report the resulting FID scores (Heusel et al., 2017) in Figure 6. Beta SS-DDPM achieves comparable quality with the Improved DDPM model, and is slightly better on fewer number of steps. The best FID score achieved by Beta SS-DDPM is 3.17 at  $T = 1000$ .

### 5. Related works

Our work builds upon Denoising Diffusion Probabilistic Models (Ho et al., 2020). Interest in diffusion models has increased recently due to their impressive results in image (Ho et al., 2020; Song et al., 2020b; Dhariwal & Nichol, 2021) and audio (Popov et al., 2021; Liu et al., 2022) generation. However, conventional diffusion models are limited to using Gaussian noise to specify generative process. These limitations and the high quality of samples has spearheaded a series of papers exploring ways to extend diffusion models to more flexible distributions of noise.

The authors of DDIM (Song et al., 2020a) proposed an approach to build an implicit diffusion model that allows to

Table 1: Experiments results. The first row is real data and the second are generated samples. For von Mises–Fisher and Dirichlet models we show two-dimensional histograms of samples. For the Wishart model we draw ellipses, corresponding to the p.d. matrices  $x_0$  and  $x_\theta$ . The darker the pixel, the more ellipses pass through that pixel.



build a non-Markovian forward process. This formulation greatly simplifies the problem of building a connection between distributions that form a forward process and marginal distributions. Later, the authors of (Zhang et al., 2022) have formulated this approach in a more general form. However, implicit diffusion models still rely on Gaussian distributions.

To the best of our knowledge, for the first time, an approach for constructing diffusion without a consecutive process was proposed in (Rissanen et al., 2022). In this work, the authors used a similar formulation of the model and an objective to build diffusion process based on blurring instead of noise injection. Later in (Daras et al., 2022; Hoogeboom & Salimans, 2022) this approach was combined with standard Gaussian diffusion.

The authors of Cold Diffusion (Bansal et al., 2022) proposed a heuristic non-probabilistic approach to reversing almost any degradation process. The authors of Flow Matching (Lipman et al., 2022) developed an alternative probabilistic framework that works with any differentiable degradation process. However, the generative process in both of these approaches is deterministic.

In (De Bortoli et al., 2022) the authors proposed an approach to build diffusion on the manifold on which the data lies by projecting the stochastic differential equation onto it. By design, Riemannian diffusion only works with continuous time diffusion, which makes this approach expensive to apply to high-dimensional data.

In (Vahdat et al., 2021) the authors proposed to run a diffu-

sion model in the latent space of a Variational Autoencoder (Kingma & Welling, 2013; Rezende et al., 2014). Extending this idea, the authors of (Kim et al., 2022) proposed to run diffusion in the latent space of a Normalizing Flow (Grathwohl et al., 2018; Chen et al., 2019). Latent diffusion is another way to apply diffusion to different domains. However, under the hood these approaches still apply a conventional Gaussian diffusion.

The authors of (Zhang & Chen, 2021) extended the idea of modifying the diffusion model latent space and proposed a way to build a fully trainable diffusion model that reduces the total number of diffusion steps due to more flexible dynamics. However, at training stage such approach requires backpropagation through the whole forward Markov process, significantly slowing down the training procedure. Moreover, the forward Markov process in (Zhang & Chen, 2021) still uses Gaussian noise.

In (Nachmani et al., 2021), the authors extend the DDPM to the case of the Gamma distribution. They demonstrate that for the Gamma diffusion, it is possible to compute the marginal distributions,  $q(x_t|x_0)$ , and the posterior distributions,  $q(x_{t-1}|x_t, x_0)$ , in a closed form. However, the resulting expressions are cumbersome, necessitating the utilization of an approximation for the variational lower bound. Furthermore, the approach employed by the authors is ad hoc and not generalizable to other cases.

## 6. Conclusion

We propose an alternative view on diffusion-like probabilistic models. We reveal the duality between star-shaped and Markov diffusion processes that allows us to go far beyond Gaussian noise by switching to a star-shaped formulation. This duality provides us with insights of how to set the noise schedules in star-shaped diffusion models regardless of the choice of the noising distribution which would be problematic otherwise. It allows us to define diffusion-like models with arbitrary noising distributions and to establish diffusion processes on specific manifolds. We propose an efficient way to construct a reverse process for such models in the case when the noising process lies in a general subset of the exponential family and show that star-shaped diffusion models can be trained on a variety of domains with different noising distributions. On image domain star-shaped model with Beta distributed noise shows comparable performance to Gaussian DDPM which is known to attain state-of-art performance on that domain. The star-shaped formulation opens new applications of diffusion-like probabilistic models, especially for data from exotic domains where domain-specific non-Gaussian diffusion is more appropriate. Any star-shaped model implicitly defines a dual Markov diffusion process in the space of tail statistics. The explicit description and analysis of this process remains an interesting open problem.

## Acknowledgements

This research was supported in part through computational resources of HPC facilities at HSE University.

## References

Arjovsky, M., Chintala, S., and Bottou, L. Wasserstein gan. arxiv 2017. *arXiv preprint arXiv:1701.07875*, 30:4, 2017.

Bansal, A., Borgnia, E., Chu, H.-M., Li, J. S., Kazemi, H., Huang, F., Goldblum, M., Geiping, J., and Goldstein, T. Cold diffusion: Inverting arbitrary image transforms without noise. *arXiv preprint arXiv:2208.09392*, 2022.

Brock, A., Donahue, J., and Simonyan, K. Large scale gan training for high fidelity natural image synthesis. *arXiv preprint arXiv:1809.11096*, 2018.

Chen, R. T., Behrmann, J., Duvenaud, D. K., and Jacobsen, J.-H. Residual flows for invertible generative modeling. *Advances in Neural Information Processing Systems*, 32, 2019.

Daras, G., Delbracio, M., Talebi, H., Dimakis, A. G., and Milanfar, P. Soft diffusion: Score matching for general corruptions. *arXiv preprint arXiv:2209.05442*, 2022.

De Bortoli, V., Mathieu, E., Hutchinson, M., Thornton, J., Teh, Y. W., and Doucet, A. Riemannian score-based generative modeling. *arXiv preprint arXiv:2202.02763*, 2022.

Dhariwal, P. and Nichol, A. Diffusion models beat gans on image synthesis. *arXiv preprint arXiv:2105.05233*, 2021.

EOSDIS. Land, atmosphere near real-time capability for eos (lance) system operated by nasa's earth science data and information system (esdis). <https://earthdata.nasa.gov/earth-observation-data/near-real-time/firms/active-fire-data>, 2020.

Goodfellow, I., Pouget-Abadie, J., Mirza, M., Xu, B., Warde-Farley, D., Ozair, S., Courville, A., and Bengio, Y. Generative adversarial nets. *Advances in neural information processing systems*, 27, 2014.

Grathwohl, W., Chen, R. T., Bettencourt, J., Sutskever, I., and Duvenaud, D. Ffjord: Free-form continuous dynamics for scalable reversible generative models. *arXiv preprint arXiv:1810.01367*, 2018.

Gulrajani, I., Ahmed, F., Arjovsky, M., Dumoulin, V., and Courville, A. C. Improved training of wasserstein gans. *Advances in neural information processing systems*, 30, 2017.

He, K., Zhang, X., Ren, S., and Sun, J. Deep residual learning for image recognition. *corr abs/1512.03385* (2015), 2015.

Heusel, M., Ramsauer, H., Unterthiner, T., Nessler, B., and Hochreiter, S. Gans trained by a two time-scale update rule converge to a local nash equilibrium. *Advances in neural information processing systems*, 30, 2017.

Ho, J., Jain, A., and Abbeel, P. Denoising diffusion probabilistic models. *arXiv preprint arXiv:2006.11239*, 2020.

Hoogeboom, E. and Salimans, T. Blurring diffusion models. *arXiv preprint arXiv:2209.05557*, 2022.

Hoogeboom, E., Nielsen, D., Jaini, P., Forré, P., and Welling, M. Argmax flows and multinomial diffusion: Learning categorical distributions. *Advances in Neural Information Processing Systems*, 34:12454–12465, 2021.

Karras, T., Laine, S., and Aila, T. A style-based generator architecture for generative adversarial networks. In *Proceedings of the IEEE/CVF conference on computer vision and pattern recognition*, pp. 4401–4410, 2019.

Karras, T., Aittala, M., Laine, S., Härkönen, E., Hellsten, J., Lehtinen, J., and Aila, T. Alias-free generative adversarial networks. *Advances in Neural Information Processing Systems*, 34, 2021.

Kim, D., Na, B., Kwon, S. J., Lee, D., Kang, W., and Moon, I.-C. Maximum likelihood training of implicit nonlinear diffusion models. *arXiv preprint arXiv:2205.13699*, 2022.

Kingma, D. P. and Ba, J. Adam: A method for stochastic optimization. In *International Conference on Learning Representations*, 2015.

Kingma, D. P. and Welling, M. Auto-encoding variational bayes. *arXiv preprint arXiv:1312.6114*, 2013.

Kingma, D. P., Salimans, T., Poole, B., and Ho, J. Variational diffusion models. *arXiv preprint arXiv:2107.00630*, 2, 2021.

Kraskov, A., Stögbauer, H., and Grassberger, P. Estimating mutual information. *Physical review E*, 69(6):066138, 2004.

Lipman, Y., Chen, R. T., Ben-Hamu, H., Nickel, M., and Le, M. Flow matching for generative modeling. *arXiv preprint arXiv:2210.02747*, 2022.

Liu, S., Su, D., and Yu, D. Diffgan-tts: High-fidelity and efficient text-to-speech with denoising diffusion gans. *arXiv preprint arXiv:2201.11972*, 2022.

Loshchilov, I. and Hutter, F. Decoupled weight decay regularization. In *International Conference on Learning Representations*.

Luo, S. and Hu, W. Diffusion probabilistic models for 3d point cloud generation. In *Proceedings of the IEEE/CVF Conference on Computer Vision and Pattern Recognition*, pp. 2837–2845, 2021.

Molchanov, D., Kharitonov, V., Sobolev, A., and Vetrov, D. Doubly semi-implicit variational inference. In *The 22nd International Conference on Artificial Intelligence and Statistics*, pp. 2593–2602. PMLR, 2019.

Nachmani, E., Roman, R. S., and Wolf, L. Denoising diffusion gamma models. *arXiv preprint arXiv:2110.05948*, 2021.

Nichol, A. and Dhariwal, P. Improved denoising diffusion probabilistic models. *arXiv preprint arXiv:2102.09672*, 2021.

Pitman, E. J. G. Sufficient statistics and intrinsic accuracy. *Mathematical Proceedings of the Cambridge Philosophical Society*, 32(4):567–579, 1936. doi: 10.1017/S0305004100019307.

Popov, V., Vovk, I., Gogoryan, V., Sadekova, T., and Kudinov, M. Grad-tts: A diffusion probabilistic model for text-to-speech. In *International Conference on Machine Learning*, pp. 8599–8608. PMLR, 2021.

Ramesh, A., Pavlov, M., Goh, G., Gray, S., Voss, C., Radford, A., Chen, M., and Sutskever, I. Zero-shot text-to-image generation. In *International Conference on Machine Learning*, pp. 8821–8831. PMLR, 2021.

Rezende, D. J., Mohamed, S., and Wierstra, D. Stochastic backpropagation and approximate inference in deep generative models. In *International conference on machine learning*, pp. 1278–1286. PMLR, 2014.

Rissanen, S., Heinonen, M., and Solin, A. Generative modelling with inverse heat dissipation. *arXiv preprint arXiv:2206.13397*, 2022.

Saharia, C., Ho, J., Chan, W., Salimans, T., Fleet, D. J., and Norouzi, M. Image super-resolution via iterative refinement. *arXiv preprint arXiv:2104.07636*, 2021.

Sohl-Dickstein, J., Weiss, E., Maheswaranathan, N., and Ganguli, S. Deep unsupervised learning using nonequilibrium thermodynamics. In *International Conference on Machine Learning*, pp. 2256–2265. PMLR, 2015.

Song, J., Meng, C., and Ermon, S. Denoising diffusion implicit models. *arXiv preprint arXiv:2010.02502*, 2020a.

Song, Y., Sohl-Dickstein, J., Kingma, D. P., Kumar, A., Ermon, S., and Poole, B. Score-based generative modeling through stochastic differential equations. *arXiv preprint arXiv:2011.13456*, 2020b.

Thanh-Tung, H. and Tran, T. Catastrophic forgetting and mode collapse in gans. In *2020 International Joint Conference on Neural Networks (IJCNN)*, pp. 1–10. IEEE, 2020.

Vahdat, A., Kreis, K., and Kautz, J. Score-based generative modeling in latent space. *Advances in Neural Information Processing Systems*, 34, 2021.

Vaswani, A., Shazeer, N., Parmar, N., Uszkoreit, J., Jones, L., Gomez, A. N., Kaiser, Ł., and Polosukhin, I. Attention is all you need. *Advances in neural information processing systems*, 30, 2017.

Xiao, Z., Kreis, K., Kautz, J., and Vahdat, A. Vaebm: A symbiosis between variational autoencoders and energy-based models. *arXiv preprint arXiv:2010.00654*, 2020.

Yin, M. and Zhou, M. Semi-implicit variational inference. In *International Conference on Machine Learning*, pp. 5660–5669. PMLR, 2018.

Zhang, L., Goldstein, M., and Ranganath, R. Understanding failures in out-of-distribution detection with deep generative models. In *International Conference on Machine Learning*, pp. 12427–12436. PMLR, 2021.

Zhang, Q. and Chen, Y. Diffusion normalizing flow. *arXiv preprint arXiv:2110.07579*, 2021.

Zhang, Q., Tao, M., and Chen, Y. gddim: Generalized denoising diffusion implicit models. *arXiv preprint arXiv:2206.05564*, 2022.

Zhao, S., Ren, H., Yuan, A., Song, J., Goodman, N., and Ermon, S. Bias and generalization in deep generative models: An empirical study. *Advances in Neural Information Processing Systems*, 31, 2018.

Zhou, L., Du, Y., and Wu, J. 3d shape generation and completion through point-voxel diffusion. In *Proceedings of the IEEE/CVF International Conference on Computer Vision*, pp. 5826–5835, 2021.

## A. Variational lower bound for the SS-DDPM model

$$\mathcal{L}^{\text{ss}}(\theta) = \mathbb{E}_{q^{\text{ss}}(x_{0:T})} \log \frac{p_{\theta}^{\text{ss}}(x_{0:T})}{q^{\text{ss}}(x_{1:T}|x_0)} = \mathbb{E}_{q^{\text{ss}}(x_{0:T})} \log \frac{p_{\theta}^{\text{ss}}(x_0|x_{1:T}) p_{\theta}^{\text{ss}}(x_T) \prod_{t=2}^T p_{\theta}^{\text{ss}}(x_{t-1}|x_{t:T})}{\prod_{t=1}^T q^{\text{ss}}(x_t|x_0)} = \quad (26)$$

$$= \mathbb{E}_{q^{\text{ss}}(x_{0:T})} \left[ \log p_{\theta}^{\text{ss}}(x_0|x_{1:T}) + \sum_{t=2}^T \log \frac{p_{\theta}^{\text{ss}}(x_{t-1}|x_{t:T})}{q^{\text{ss}}(x_{t-1}|x_0)} + \log \frac{p_{\theta}^{\text{ss}}(x_T)}{q^{\text{ss}}(x_T|x_0)} \right] = \quad (27)$$

$$= \mathbb{E}_{q^{\text{ss}}(x_{0:T})} \left[ \log p_{\theta}^{\text{ss}}(x_0|x_{1:T}) - \sum_{t=2}^T D_{KL}(q^{\text{ss}}(x_{t-1}|x_0) \| p_{\theta}^{\text{ss}}(x_{t-1}|x_{t:T})) \right] \quad (28)$$

## B. True reverse process for Markovian and Star-Shaped DDPM

If the forward process is Markovian, the corresponding true reverse process is Markovian too:

$$q^{\text{DDPM}}(x_{t-1}|x_{t:T}) = \frac{q^{\text{DDPM}}(x_{t-1:T})}{q^{\text{DDPM}}(x_{t:T})} = \frac{q^{\text{DDPM}}(x_{t-1}) q^{\text{DDPM}}(x_t|x_{t-1}) \overbrace{\prod_{s=t+1}^T q^{\text{DDPM}}(x_s|x_{s-1})}^{\widehat{q^{\text{DDPM}}(x_s|x_{s-1})}}}{q^{\text{DDPM}}(x_t) \underbrace{\prod_{s=t+1}^T q^{\text{DDPM}}(x_s|x_{s-1})}_{\widehat{q^{\text{DDPM}}(x_s|x_{s-1})}}} = q^{\text{DDPM}}(x_{t-1}|x_t) \quad (29)$$

$$q^{\text{DDPM}}(x_{0:T}) = q(x_0) \prod_{t=1}^T q^{\text{DDPM}}(x_t|x_{t-1}) = q^{\text{DDPM}}(x_T) \prod_{t=1}^T q^{\text{DDPM}}(x_{t-1}|x_{t:T}) = q^{\text{DDPM}}(x_T) \prod_{t=1}^T q^{\text{DDPM}}(x_{t-1}|x_t) \quad (30)$$

For star-shaped models, however, the reverse process has a general structure that cannot be reduced further:

$$q^{\text{ss}}(x_{0:T}) = q(x_0) \prod_{t=1}^T q^{\text{ss}}(x_t|x_0) = q^{\text{ss}}(x_T) \prod_{t=1}^T q^{\text{ss}}(x_{t-1}|x_{t:T}) \quad (31)$$

In this case a Markovian reverse process can be a very poor approximation to the true reverse process. Choosing such approximation adds an irreducible gap to the variational lower bound:

$$\mathcal{L}_{\text{Markov}}^{\text{ss}}(\theta) = \mathbb{E}_{q^{\text{ss}}(x_{0:T})} \log \frac{p_{\theta}(x_T) \prod_{t=1}^T p_{\theta}(x_{t-1}|x_t)}{q^{\text{ss}}(x_{1:T}|x_0)} = \quad (32)$$

$$= \mathbb{E}_{q^{\text{ss}}(x_{0:T})} \log \frac{p_{\theta}(x_T) \prod_{t=1}^T p_{\theta}(x_{t-1}|x_t) q(x_0) \prod_{t=1}^T q^{\text{ss}}(x_{t-1}|x_t)}{q^{\text{ss}}(x_T) \prod_{t=1}^T q^{\text{ss}}(x_{t-1}|x_{t:T}) \prod_{t=1}^T} = \quad (33)$$

$$= \mathbb{E}_{q^{\text{ss}}(x_{0:T})} \left[ \underbrace{\log q(x_0) - D_{KL}(q^{\text{ss}}(x_T) \| p_{\theta}(x_T)) - \sum_{t=1}^T D_{KL}(q^{\text{ss}}(x_{t-1}|x_t) \| p_{\theta}(x_{t-1}|x_t))}_{\text{Reducible}} - \right. \quad (34)$$

$$\left. \underbrace{\sum_{t=1}^T D_{KL}(q^{\text{ss}}(x_{t-1}|x_{t:T}) \| q^{\text{ss}}(x_{t-1}|x_t))}_{\text{Irreducible}} \right] \quad (35)$$

Intuitively, there is little information shared between  $x_{t-1}$  and  $x_t$ , as they are conditionally independent given  $x_0$ . Therefore, we would expect the distribution  $q^{\text{ss}}(x_{t-1}|x_t)$  to have a much higher entropy than the distribution  $q^{\text{ss}}(x_{t-1}|x_{t:T})$ , making the irreducible gap (35) large. The dramatic effect of this gap is illustrated in Figure 3.

This gap can also be computed analytically for Gaussian DDPMs when the data is coming from a standard Gaussian distribution  $q(x_0) = \mathcal{N}(x_0; 0, 1)$ . According to (34–35), the best Markovian reverse process in this case is  $p_\theta(x_{t-1}|x_t) = q^{\text{ss}}(x_{t-1}|x_t)$ . It results in the following value of the variational lower bound:

$$\mathcal{L}_{\text{Markov}}^{\text{ss}} = -\mathcal{H}[q(x_0)] + \mathcal{H}[q^{\text{ss}}(x_{0:T})] - \mathcal{H}[q^{\text{ss}}(x_T)] - \frac{1}{2} \sum_{t=1}^T [1 + \log(2\pi(1 - \bar{\alpha}_{t-1}^{\text{ss}} \bar{\alpha}_t^{\text{ss}}))] \quad (36)$$

If the reverse process is matched exactly (and has a general structure), the variational lower bound reduces to the negative entropy of the data distribution:

$$\mathcal{L}_*^{\text{ss}} = \mathbb{E}_{q^{\text{ss}}(x_{0:T})} \log \frac{p_*^{\text{ss}}(x_{0:T})}{q^{\text{ss}}(x_{1:T}|x_0)} = \quad (37)$$

$$= \mathbb{E}_{q^{\text{ss}}(x_{0:T})} \log \frac{q^{\text{ss}}(x_{0:T})}{q^{\text{ss}}(x_{1:T}|x_0)} = \quad (38)$$

$$= \mathbb{E}_{q(x_0)} \log q(x_0) = -\frac{1}{2} \log(2\pi) - \frac{1}{2} \quad (39)$$

As shown in Figure 7, the Markovian approximation adds a substantial irreducible gap to the variational lower bound.

## C. Proof of Theorem 1

**Theorem 1.** *Given*

$$q^{\text{ss}}(x_t|x_0) = h_t(x_t) \exp \{ \eta_t(x_0)^\top \mathcal{T}(x_t) - \Omega_t(x_0) \} \quad (14)$$

$$\eta_t(x_0) = A_t f(x_0) + b_t \quad (15)$$

$$G_t = \mathcal{G}_t(x_{t:T}) = \sum_{s=t}^T A_s^\top \mathcal{T}(x_s) \quad (16)$$

the following holds:

$$q^{\text{ss}}(x_{t-1}|x_{t:T}) = q^{\text{ss}}(x_{t-1}|G_t) \quad (17)$$

*Proof.*

$$q^{\text{ss}}(x_{t-1}|x_{t:T}) = \int q^{\text{ss}}(x_{t-1}|x_0) q^{\text{ss}}(x_0|x_{t:T}) dx_0 \quad (40)$$

$$q^{\text{ss}}(x_0|x_{t:T}) = \frac{q(x_0) \prod_{s=t}^T q^{\text{ss}}(x_s|x_0)}{q^{\text{ss}}(x_{t:T})} = \frac{q(x_0)}{q^{\text{ss}}(x_{t:T})} \left( \prod_{s=t}^T h_s(x_s) \right) \exp \left\{ \sum_{s=t}^T (\eta_s(x_0)^\top \mathcal{T}(x_s) - \Omega_s(x_0)) \right\} = \quad (41)$$

$$= \frac{q(x_0)}{q^{\text{ss}}(x_{t:T})} \left( \prod_{s=t}^T h_s(x_s) \right) \exp \left\{ \sum_{s=t}^T ((A_s f(x_0) + b_s)^\top \mathcal{T}(x_s) - \Omega_s(x_0)) \right\} = \quad (42)$$

$$= \frac{q(x_0)}{q^{\text{ss}}(x_{t:T})} \left( \prod_{s=t}^T h_s(x_s) \right) \exp \left\{ f(x_0)^\top \sum_{s=t}^T A_s^\top \mathcal{T}(x_s) + \sum_{s=t}^T (b_s^\top \mathcal{T}(x_s) - \Omega_s(x_0)) \right\} = \quad (43)$$

$$= \frac{q(x_0)}{q^{\text{ss}}(x_{t:T})} \left( \prod_{s=t}^T h_s(x_s) \right) \exp \left\{ f(x_0)^\top G_t + \sum_{s=t}^T (b_s^\top \mathcal{T}(x_s) - \Omega_s(x_0)) \right\} = \quad (44)$$

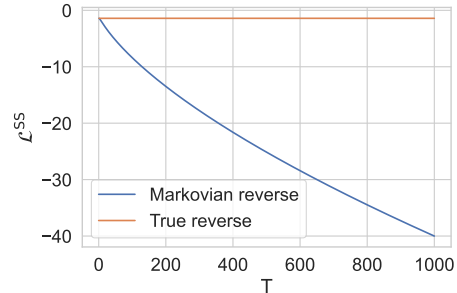


Figure 7: Variational lower bound for a Gaussian Star-Shaped DDPM model computed with the true reverse process and with the best Markovian approximation.

$$= \frac{q(x_0) \exp \left\{ f(x_0)^\top G_t - \sum_{s=t}^T \Omega_s(x_0) \right\}}{\int q(x_0) \exp \left\{ f(x_0)^\top G_t - \sum_{s=t}^T \Omega_s(x_0) \right\} dG_t} = q^{\text{ss}}(x_0|G_t) \quad (45)$$

$$q^{\text{ss}}(x_{t-1}|x_{t:T}) = \int q^{\text{ss}}(x_{t-1}|x_0) q^{\text{ss}}(x_0|x_{t:T}) dx_0 = \int q^{\text{ss}}(x_{t-1}|x_0) q^{\text{ss}}(x_0|G_t) dx_0 = q^{\text{ss}}(x_{t-1}|G_t) \quad (46)$$

□

## D. Gaussian SS-DDPM is equivalent to Gaussian DDPM

**Theorem 2.** Let  $\bar{\alpha}_t^{\text{DDPM}}$  define the noising schedule for a DDPM model (1–2) via  $\beta_t = (\bar{\alpha}_{t-1}^{\text{DDPM}} - \bar{\alpha}_t^{\text{DDPM}})/\bar{\alpha}_{t-1}^{\text{DDPM}}$ . Let  $q^{\text{ss}}(x_{0:T})$  be a Gaussian SS-DDPM forward process with the following noising schedule and tail statistic:

$$q^{\text{ss}}(x_t|x_0) = \mathcal{N} \left( x_t; \sqrt{\bar{\alpha}_t^{\text{ss}}} x_0, 1 - \bar{\alpha}_t^{\text{ss}} \right), \quad (22)$$

$$\mathcal{G}_t(x_{t:T}) = \frac{1 - \bar{\alpha}_t^{\text{DDPM}}}{\sqrt{\bar{\alpha}_t^{\text{DDPM}}}} \sum_{s=t}^T \frac{\sqrt{\bar{\alpha}_s^{\text{ss}}} x_s}{1 - \bar{\alpha}_s^{\text{ss}}}, \text{ where} \quad (23)$$

$$\frac{\bar{\alpha}_t^{\text{ss}}}{1 - \bar{\alpha}_t^{\text{ss}}} = \frac{\bar{\alpha}_t^{\text{DDPM}}}{1 - \bar{\alpha}_t^{\text{DDPM}}} - \frac{\bar{\alpha}_{t+1}^{\text{DDPM}}}{1 - \bar{\alpha}_{t+1}^{\text{DDPM}}}. \quad (24)$$

Then the tail statistic  $G_t$  follows a Gaussian DDPM noising process  $q^{\text{DDPM}}(x_{0:T})|_{x_{1:T}=G_{1:T}}$  defined by the schedule  $\bar{\alpha}_t^{\text{DDPM}}$ . Moreover, the corresponding reverse processes and VLB objectives are also equivalent.

*Proof.* First, let us remind the necessary definitions and expressions used in the Gaussian DDPM model (Ho et al., 2020).

$$q^{\text{DDPM}}(x_{0:T}) = q(x_0) \prod_{i=1}^T q^{\text{DDPM}}(x_t|x_{t-1}) \quad (47)$$

$$q^{\text{DDPM}}(x_t|x_{t-1}) = \mathcal{N} \left( x_t; \sqrt{1 - \beta_t} x_{t-1}, \beta_t \mathbf{I} \right) \quad (48)$$

$$\alpha_s^{\text{DDPM}} = 1 - \beta_s^{\text{DDPM}} \quad (49)$$

$$\bar{\alpha}_t^{\text{DDPM}} = \prod_{s=1}^t \alpha_s^{\text{DDPM}} \quad (50)$$

$$q^{\text{DDPM}}(x_t|x_0) = \mathcal{N} \left( x_t; \sqrt{\bar{\alpha}_t^{\text{DDPM}}} x_0, (1 - \bar{\alpha}_t^{\text{DDPM}}) \mathbf{I} \right) \quad (51)$$

$$\tilde{\mu}_t(x_t, x_0) = \frac{\sqrt{\bar{\alpha}_{t-1}^{\text{DDPM}}} \beta_t}{1 - \bar{\alpha}_t^{\text{DDPM}}} x_0 + \frac{\sqrt{\bar{\alpha}_t^{\text{DDPM}}} (1 - \bar{\alpha}_{t-1}^{\text{DDPM}})}{1 - \bar{\alpha}_t^{\text{DDPM}}} x_t \quad (52)$$

$$\tilde{\beta}_t^{\text{DDPM}} = \frac{1 - \bar{\alpha}_{t-1}^{\text{DDPM}}}{1 - \bar{\alpha}_t^{\text{DDPM}}} \beta_t \quad (53)$$

$$q^{\text{DDPM}}(x_{t-1}|x_t, x_0) = \mathcal{N} \left( x_{t-1}; \tilde{\mu}_t(x_t, x_0), \tilde{\beta}_t^{\text{DDPM}} \mathbf{I} \right) \quad (54)$$

$$p_{\theta}^{\text{DDPM}}(x_{0:T}) = q^{\text{DDPM}}(x_T) \prod_{i=1}^T p_{\theta}^{\text{DDPM}}(x_{t-1}|x_t) \quad (55)$$

$$p_{\theta}^{\text{DDPM}}(x_{t-1}|x_t) = \mathcal{N} \left( x_{t-1}; \tilde{\mu}_t(x_t, x_{\theta}^{\text{DDPM}}(x_t, t)), \tilde{\beta}_t^{\text{DDPM}} \mathbf{I} \right) \quad (56)$$

In this notation the variational lower bound for DDPM can be written as follows (here we omit the term corresponding to  $x_T$  because it's either zero or a small constant):

$$\mathcal{L}^{\text{DDPM}}(\theta) = \mathbb{E}_{q^{\text{DDPM}}(x_{0:T})} \left[ \log p_{\theta}^{\text{DDPM}}(x_0|x_1) - \sum_{t=2}^T D_{KL} (q^{\text{DDPM}}(x_{t-1}|x_t, x_0) \parallel p_{\theta}^{\text{DDPM}}(x_{t-1}|x_t)) \right] = \quad (57)$$

$$= \mathbb{E}_{q^{\text{DDPM}}(x_{0:T})} \left[ \log p_{\theta}^{\text{DDPM}}(x_0|x_1) - \sum_{t=2}^T D_{KL} \left( q^{\text{DDPM}}(x_{t-1}|x_t, x_0) \parallel q^{\text{DDPM}}(x_{t-1}|x_t, x_0) \big|_{x_0=x_{\theta}^{\text{DDPM}}(x_t, t)} \right) \right] \quad (58)$$

$$D_{KL} \left( q^{\text{DDPM}}(x_{t-1}|x_t, x_0) \parallel q^{\text{DDPM}}(x_{t-1}|x_t, x_0) \big|_{x_0=x_{\theta}^{\text{DDPM}}(x_t, t)} \right) = \frac{\left( \frac{\sqrt{\alpha_{t-1}^{\text{DDPM}} \beta_t^{\text{DDPM}}}}{1-\bar{\alpha}_t^{\text{DDPM}}} (x_0 - x_{\theta}^{\text{DDPM}}(x_t, t)) \right)^2}{2\tilde{\beta}_t^{\text{DDPM}}} \quad (59)$$

For convenience, we additionally define  $\bar{\alpha}_{T+1}^{\text{DDPM}} = 0$ . Since all the involved distributions are typically isotropic, we consider a one-dimensional case without the loss of generality.

First, we show that the forward processes  $q^{\text{ss}}(x_0, G_{1:T})$  and  $q^{\text{DDPM}}(x_{0:T})$  are equivalent.

$$G_t = \frac{1 - \bar{\alpha}_t^{\text{DDPM}}}{\sqrt{\bar{\alpha}_t^{\text{DDPM}}}} \sum_{s=t}^T \frac{\sqrt{\bar{\alpha}_s^{\text{ss}}} x_s}{1 - \bar{\alpha}_s^{\text{ss}}} \quad (60)$$

Since  $G_t$  is a linear combination of independent (given  $x_0$ ) Gaussian random variables, it's distribution (given  $x_0$ ) is also Gaussian. All the terms conveniently cancel out, and we recover the same form as the forward process of DDPM.

$$q^{\text{ss}}(G_t|x_0) = \mathcal{N} \left( G_t; \frac{1 - \bar{\alpha}_t^{\text{DDPM}}}{\sqrt{\bar{\alpha}_t^{\text{DDPM}}}} \sum_{s=t}^T \frac{\bar{\alpha}_s^{\text{ss}} x_0}{1 - \bar{\alpha}_s^{\text{ss}}}; \left( \frac{1 - \bar{\alpha}_t^{\text{DDPM}}}{\sqrt{\bar{\alpha}_t^{\text{DDPM}}}} \right)^2 \sum_{s=t}^T \left( \frac{\bar{\alpha}_s^{\text{ss}}}{(1 - \bar{\alpha}_s^{\text{ss}})^2} (1 - \bar{\alpha}_s^{\text{ss}}) \right) \right) = \quad (61)$$

$$= \mathcal{N} \left( G_t; \frac{1 - \bar{\alpha}_t^{\text{DDPM}}}{\sqrt{\bar{\alpha}_t^{\text{DDPM}}}} \frac{\bar{\alpha}_t^{\text{DDPM}}}{1 - \bar{\alpha}_t^{\text{DDPM}}} x_0; \left( \frac{1 - \bar{\alpha}_t^{\text{DDPM}}}{\sqrt{\bar{\alpha}_t^{\text{DDPM}}}} \right)^2 \frac{\bar{\alpha}_t^{\text{DDPM}}}{1 - \bar{\alpha}_t^{\text{DDPM}}} \right) = \quad (62)$$

$$= \mathcal{N} \left( G_t; \sqrt{\bar{\alpha}_t^{\text{DDPM}}} x_0; (1 - \bar{\alpha}_t^{\text{DDPM}}) \right) = q^{\text{DDPM}}(x_t|x_0)|_{x_t=G_t} \quad (63)$$

Since both processes share the same  $q(x_0)$ , and have the same Markovian structure, matching these marginals sufficiently shows that the processes are equivalent:

$$q^{\text{ss}}(x_0, G_{1:T}) = q^{\text{DDPM}}(x_{0:T})|_{x_{1:T}=G_{1:T}} \quad (64)$$

Consequently, the posteriors are matching too:

$$q^{\text{ss}}(G_{t-1}|G_t, x_0) = q^{\text{DDPM}}(x_{t-1}|x_t, x_0)|_{x_{t-1,t}=G_{t-1,t}} \quad (65)$$

Next, we show that the reverse processes  $p_{\theta}^{\text{ss}}(G_{t-1}|G_t)$  and  $p_{\theta}^{\text{DDPM}}(x_{t-1}|x_t)$  are the same. Since  $G_t$  in SS-DDPM is the same as  $x_t$  in DDPM, we can assume the predictive models  $x_{\theta}^{\text{ss}}(G_t, t)$  and  $x_{\theta}^{\text{DDPM}}(x_t, t)$  to coincide at  $x_t = G_t$ .

$$G_{t-1} = \frac{1 - \bar{\alpha}_{t-1}^{\text{DDPM}}}{\sqrt{\bar{\alpha}_{t-1}^{\text{DDPM}}}} \sum_{s=t-1}^T \frac{\sqrt{\bar{\alpha}_s^{\text{ss}}} x_s}{1 - \bar{\alpha}_s^{\text{ss}}} = \frac{1 - \bar{\alpha}_{t-1}^{\text{DDPM}}}{\sqrt{\bar{\alpha}_{t-1}^{\text{DDPM}}}} \frac{\sqrt{\bar{\alpha}_{t-1}^{\text{ss}}} x_{t-1}}{1 - \bar{\alpha}_{t-1}^{\text{ss}}} + \frac{1 - \bar{\alpha}_{t-1}^{\text{DDPM}}}{\sqrt{\bar{\alpha}_{t-1}^{\text{DDPM}}}} \frac{\sqrt{\bar{\alpha}_t^{\text{DDPM}}} G_t}{1 - \bar{\alpha}_t^{\text{DDPM}}} = \quad (66)$$

$$= \frac{1 - \bar{\alpha}_{t-1}^{\text{DDPM}}}{\sqrt{\bar{\alpha}_{t-1}^{\text{DDPM}}}} \sum_{s=t-1}^T \frac{\sqrt{\bar{\alpha}_s^{\text{ss}}} x_s}{1 - \bar{\alpha}_s^{\text{ss}}} = \frac{1 - \bar{\alpha}_{t-1}^{\text{DDPM}}}{\sqrt{\bar{\alpha}_{t-1}^{\text{DDPM}}}} \frac{\sqrt{\bar{\alpha}_{t-1}^{\text{ss}}} x_{t-1}}{1 - \bar{\alpha}_{t-1}^{\text{ss}}} + \frac{\sqrt{\bar{\alpha}_t^{\text{DDPM}}} (1 - \bar{\alpha}_{t-1}^{\text{DDPM}})}{1 - \bar{\alpha}_t^{\text{DDPM}}} G_t, \quad (67)$$

where  $x_{t-1} \sim p_{\theta}^{\text{ss}}(x_{t-1}|G_t) = q^{\text{ss}}(x_{t-1}|x_0)|_{x_0=x_{\theta}(G_t, t)}$ . Therefore,  $p_{\theta}^{\text{ss}}(G_{t-1}|G_t)$  is also a Gaussian distribution. Let's take care of the mean first:

$$\mathbb{E}_{p_{\theta}^{\text{ss}}(G_{t-1}|G_t)} G_{t-1} = \frac{1 - \bar{\alpha}_{t-1}^{\text{DDPM}}}{\sqrt{\bar{\alpha}_{t-1}^{\text{DDPM}}}} \frac{\bar{\alpha}_{t-1}^{\text{ss}}}{1 - \bar{\alpha}_{t-1}^{\text{ss}}} x_{\theta}(G_t, t) + \frac{\sqrt{\bar{\alpha}_t^{\text{DDPM}}} (1 - \bar{\alpha}_{t-1}^{\text{DDPM}})}{1 - \bar{\alpha}_t^{\text{DDPM}}} G_t = \quad (68)$$

$$= \frac{1 - \bar{\alpha}_{t-1}^{\text{DDPM}}}{\sqrt{\bar{\alpha}_{t-1}^{\text{DDPM}}}} \left( \frac{\bar{\alpha}_{t-1}^{\text{DDPM}}}{1 - \bar{\alpha}_{t-1}^{\text{DDPM}}} - \frac{\bar{\alpha}_t^{\text{DDPM}}}{1 - \bar{\alpha}_t^{\text{DDPM}}} \right) x_\theta(G_t, t) + \frac{\sqrt{\alpha_t^{\text{DDPM}}(1 - \bar{\alpha}_{t-1}^{\text{DDPM}})}}{1 - \bar{\alpha}_t^{\text{DDPM}}} G_t = \quad (69)$$

$$= \left( \sqrt{\bar{\alpha}_{t-1}^{\text{DDPM}}} - \frac{(1 - \bar{\alpha}_{t-1}^{\text{DDPM}})\sqrt{\bar{\alpha}_{t-1}^{\text{DDPM}}}\alpha_t^{\text{DDPM}}}{1 - \bar{\alpha}_t^{\text{DDPM}}} \right) x_\theta(G_t, t) + \frac{\sqrt{\alpha_t^{\text{DDPM}}(1 - \bar{\alpha}_{t-1}^{\text{DDPM}})}}{1 - \bar{\alpha}_t^{\text{DDPM}}} G_t = \quad (70)$$

$$= \left( \frac{1 - \bar{\alpha}_t^{\text{DDPM}} - (1 - \bar{\alpha}_{t-1}^{\text{DDPM}})\alpha_t^{\text{DDPM}}}{1 - \bar{\alpha}_t^{\text{DDPM}}} \right) \sqrt{\bar{\alpha}_{t-1}^{\text{DDPM}}} x_\theta(G_t, t) + \frac{\sqrt{\alpha_t^{\text{DDPM}}(1 - \bar{\alpha}_{t-1}^{\text{DDPM}})}}{1 - \bar{\alpha}_t^{\text{DDPM}}} G_t = \quad (71)$$

$$= \left( \frac{1 - \bar{\alpha}_t^{\text{DDPM}} - \alpha_t^{\text{DDPM}} + \bar{\alpha}_t^{\text{DDPM}}}{1 - \bar{\alpha}_t^{\text{DDPM}}} \right) \sqrt{\bar{\alpha}_{t-1}^{\text{DDPM}}} x_\theta(G_t, t) + \frac{\sqrt{\alpha_t^{\text{DDPM}}(1 - \bar{\alpha}_{t-1}^{\text{DDPM}})}}{1 - \bar{\alpha}_t^{\text{DDPM}}} G_t = \quad (72)$$

$$= \frac{\sqrt{\bar{\alpha}_{t-1}^{\text{DDPM}}}\beta_t}{1 - \bar{\alpha}_t^{\text{DDPM}}} x_\theta(G_t, t) + \frac{\sqrt{\alpha_t^{\text{DDPM}}(1 - \bar{\alpha}_{t-1}^{\text{DDPM}})}}{1 - \bar{\alpha}_t^{\text{DDPM}}} G_t \quad (73)$$

Now, let's derive the variance:

$$\mathbb{D}_{p_\theta^{\text{SS}}(G_{t-1}|G_t)} G_{t-1} = \left( \frac{1 - \bar{\alpha}_{t-1}^{\text{DDPM}}}{\sqrt{\bar{\alpha}_{t-1}^{\text{DDPM}}}} \frac{\sqrt{\alpha_{t-1}^{\text{SS}}}}{1 - \bar{\alpha}_{t-1}^{\text{SS}}} \right)^2 (1 - \bar{\alpha}_{t-1}^{\text{SS}}) = \quad (74)$$

$$= \left( \frac{1 - \bar{\alpha}_{t-1}^{\text{DDPM}}}{\sqrt{\bar{\alpha}_{t-1}^{\text{DDPM}}}} \sqrt{\frac{\bar{\alpha}_{t-1}^{\text{SS}}}{1 - \bar{\alpha}_{t-1}^{\text{SS}}}} \right)^2 = \frac{(1 - \bar{\alpha}_{t-1}^{\text{DDPM}})^2}{\bar{\alpha}_{t-1}^{\text{DDPM}}} \frac{\bar{\alpha}_{t-1}^{\text{SS}}}{1 - \bar{\alpha}_{t-1}^{\text{SS}}} = \frac{(1 - \bar{\alpha}_{t-1}^{\text{DDPM}})^2}{\bar{\alpha}_{t-1}^{\text{DDPM}}} \left( \frac{\bar{\alpha}_{t-1}^{\text{DDPM}}}{1 - \bar{\alpha}_{t-1}^{\text{DDPM}}} - \frac{\bar{\alpha}_t^{\text{DDPM}}}{1 - \bar{\alpha}_t^{\text{DDPM}}} \right) = \quad (75)$$

$$= (1 - \bar{\alpha}_{t-1}^{\text{DDPM}}) \left( 1 - \frac{(1 - \bar{\alpha}_{t-1}^{\text{DDPM}})\alpha_t^{\text{DDPM}}}{1 - \bar{\alpha}_t^{\text{DDPM}}} \right) = \frac{(1 - \bar{\alpha}_{t-1}^{\text{DDPM}})(1 - \bar{\alpha}_t^{\text{DDPM}} - (1 - \bar{\alpha}_{t-1}^{\text{DDPM}})\alpha_t^{\text{DDPM}})}{1 - \bar{\alpha}_t^{\text{DDPM}}} = \quad (76)$$

$$= \frac{1 - \bar{\alpha}_{t-1}^{\text{DDPM}}}{1 - \bar{\alpha}_t^{\text{DDPM}}} (1 - \bar{\alpha}_t^{\text{DDPM}} - \alpha_t^{\text{DDPM}} + \bar{\alpha}_t^{\text{DDPM}}) = \frac{1 - \bar{\alpha}_{t-1}^{\text{DDPM}}}{1 - \bar{\alpha}_t^{\text{DDPM}}} \beta_t^{\text{DDPM}} = \tilde{\beta}_t^{\text{DDPM}} \quad (77)$$

Therefore,

$$p_\theta^{\text{SS}}(G_{t-1}|G_t) = \mathcal{N} \left( G_{t-1}; \frac{\sqrt{\bar{\alpha}_{t-1}^{\text{DDPM}}}\beta_t}{1 - \bar{\alpha}_t^{\text{DDPM}}} x_\theta(G_t, t) + \frac{\sqrt{\alpha_t^{\text{DDPM}}(1 - \bar{\alpha}_{t-1}^{\text{DDPM}})}}{1 - \bar{\alpha}_t^{\text{DDPM}}} G_t, \tilde{\beta}_t^{\text{DDPM}} \right) = p_\theta^{\text{DDPM}}(x_{t-1}|x_t)|_{x_{t-1,t}=G_{t-1,t}} \quad (78)$$

Finally, we show that variational lower bounds are the same.

$$\mathcal{L}^{\text{SS}}(\theta) = \mathbb{E}_{q^{\text{SS}}(x_{0:T})} \left[ \log p_\theta^{\text{SS}}(x_0|G_1) - \sum_{t=2}^T D_{KL} (q^{\text{SS}}(x_{t-1}|x_0) \| p_\theta^{\text{SS}}(x_{t-1}|G_t)) \right] = \quad (79)$$

$$= \mathbb{E}_{q^{\text{SS}}(x_{0:T})} \left[ \log p_\theta^{\text{SS}}(x_0|G_1) - \sum_{t=2}^T D_{KL} \left( q^{\text{SS}}(x_{t-1}|x_0) \middle\| q^{\text{SS}}(x_{t-1}|x_0)|_{x_0=x_\theta(G_t, t)} \right) \right] \quad (80)$$

Since  $G_1$  from the star-shaped model is the same as  $x_1$  from the DDPM model, the first term  $\log p_\theta^{\text{SS}}(x_0|G_1)$  coincides with  $\log p_\theta^{\text{DDPM}}(x_0|x_1)|_{x_1=G_1}$ .

$$D_{KL} \left( q^{\text{SS}}(x_{t-1}|x_0) \middle\| q^{\text{SS}}(x_{t-1}|x_0)|_{x_0=x_\theta(G_t, t)} \right) = \frac{(\sqrt{\alpha_{t-1}^{\text{SS}}}(x_0 - x_\theta(G_t, t)))^2}{2(1 - \bar{\alpha}_{t-1}^{\text{SS}})} = \quad (81)$$

$$= \frac{\bar{\alpha}_{t-1}^{\text{SS}}}{2(1 - \bar{\alpha}_{t-1}^{\text{SS}})} (x_0 - x_\theta(G_t, t))^2 = \frac{1}{2} \left( \frac{\bar{\alpha}_{t-1}^{\text{DDPM}}}{1 - \bar{\alpha}_{t-1}^{\text{DDPM}}} - \frac{\bar{\alpha}_t^{\text{DDPM}}}{1 - \bar{\alpha}_t^{\text{DDPM}}} \right) (x_0 - x_\theta(G_t, t))^2 = \quad (82)$$

$$= \frac{1}{2} \frac{\bar{\alpha}_{t-1}^{\text{DDPM}} - \bar{\alpha}_t^{\text{DDPM}}}{(1 - \bar{\alpha}_{t-1}^{\text{DDPM}})(1 - \bar{\alpha}_t^{\text{DDPM}})} (x_0 - x_\theta(G_t, t))^2 = \frac{1}{2} \frac{\bar{\alpha}_{t-1}^{\text{DDPM}} \beta_t^{\text{DDPM}}}{(1 - \bar{\alpha}_{t-1}^{\text{DDPM}})(1 - \bar{\alpha}_t^{\text{DDPM}})} (x_0 - x_\theta(G_t, t))^2 = \quad (83)$$

$$= \frac{\bar{\alpha}_{t-1}^{\text{DDPM}} \beta_t^{\text{DDPM}} (x_0 - x_\theta^{\text{DDPM}}(x_t, t))^2}{2(1 - \bar{\alpha}_{t-1}^{\text{DDPM}})(1 - \bar{\alpha}_t^{\text{DDPM}})} = \frac{\frac{\bar{\alpha}_{t-1}^{\text{DDPM}} (\beta_t^{\text{DDPM}})^2}{(1 - \bar{\alpha}_t^{\text{DDPM}})^2} (x_0 - x_\theta^{\text{DDPM}}(x_t, t))^2}{2 \frac{1 - \bar{\alpha}_{t-1}^{\text{DDPM}}}{1 - \bar{\alpha}_t^{\text{DDPM}}} \beta_t^{\text{DDPM}}} = \quad (84)$$

$$= \frac{\left( \frac{\sqrt{\bar{\alpha}_{t-1}^{\text{DDPM}} \beta_t^{\text{DDPM}}}}{1 - \bar{\alpha}_t^{\text{DDPM}}} (x_0 - x_\theta^{\text{DDPM}}(x_t, t)) \right)^2}{2 \tilde{\beta}_t^{\text{DDPM}}} = D_{KL} \left( q^{\text{DDPM}}(x_{t-1} | x_t, x_0) \parallel q^{\text{DDPM}}(x_{t-1} | x_t, x_0) \big|_{x_0=x_\theta^{\text{DDPM}}(x_t, t)} \right) \quad (85)$$

Therefore, we finally obtain  $\mathcal{L}^{\text{SS}}(\theta) = \mathcal{L}^{\text{DDPM}}(\theta)$ .  $\square$

## E. SS-DDPM in different families

The main principles for designing a SS-DDPM model are similar to designing a DDPM model. When  $t$  goes to zero, we wish to recover a Dirac's delta, centered at  $x_0$ :

$$q^{\text{SS}}(x_t | x_0) \xrightarrow[t \rightarrow 0]{} \delta(x_t - x_0) \quad (86)$$

When  $t$  goes to  $T$ , we wish to obtain some standard distribution that doesn't depend on  $x_0$ :

$$q^{\text{SS}}(x_t | x_0) \xrightarrow[t \rightarrow T]{} q_T^{\text{SS}}(x_T) \quad (87)$$

In exponential families with linear parameterization of the natural parameter  $\eta_t(x_0) = a_t f(x_0) + b_t$ , we can define the schedule by choosing the parameters  $a_t$  and  $b_t$  that satisfy the conditions (86–87). After that we can use the Theorem 1 to define the tail statistic  $\mathcal{G}_t(x_{t:T})$  using the sufficient statistic  $\mathcal{T}(x_t)$  of the corresponding family. However, as shown in the following sections, in some cases linear parameterization admits a simpler sufficient tail statistic.

The following sections contain examples of defining the SS-DDPM model for different families. These results are summarized in Table 2.

### E.1. Gaussian

$$q^{\text{SS}}(x_t | x_0) = \mathcal{N} \left( x_t; \sqrt{\bar{\alpha}_t^{\text{SS}}} x_0, (1 - \bar{\alpha}_t^{\text{SS}}) I \right) \quad (88)$$

Since Gaussian SS-DDPM is equivalent to a Markovian DDPM, it is natural to directly reuse the schedule from a Markovian DDPM. As we show in Theorem 2, given a Markovian DDPM defined by  $\bar{\alpha}_t^{\text{DDPM}}$ , the following parameterization will produce the same process in the space of tail statistics:

$$\frac{\bar{\alpha}_t^{\text{SS}}}{1 - \bar{\alpha}_t^{\text{SS}}} = \frac{\bar{\alpha}_t^{\text{DDPM}}}{1 - \bar{\alpha}_t^{\text{DDPM}}} - \frac{\bar{\alpha}_{t+1}^{\text{DDPM}}}{1 - \bar{\alpha}_{t+1}^{\text{DDPM}}} \quad (89)$$

$$\mathcal{G}_t(x_{t:T}) = \frac{1 - \bar{\alpha}_t^{\text{DDPM}}}{\sqrt{\bar{\alpha}_t^{\text{DDPM}}}} \sum_{s=t}^T \frac{\sqrt{\bar{\alpha}_s^{\text{SS}}} x_s}{1 - \bar{\alpha}_s^{\text{SS}}} \quad (90)$$

The KL divergence is computed as follows:

$$D_{KL} (q^{\text{SS}}(x_t | x_0) \parallel p_\theta^{\text{SS}}(x_t | G_t)) = \frac{\bar{\alpha}_t^{\text{SS}} (x_0 - x_\theta(G_t, t))^2}{2(1 - \bar{\alpha}_t^{\text{SS}})} \quad (91)$$

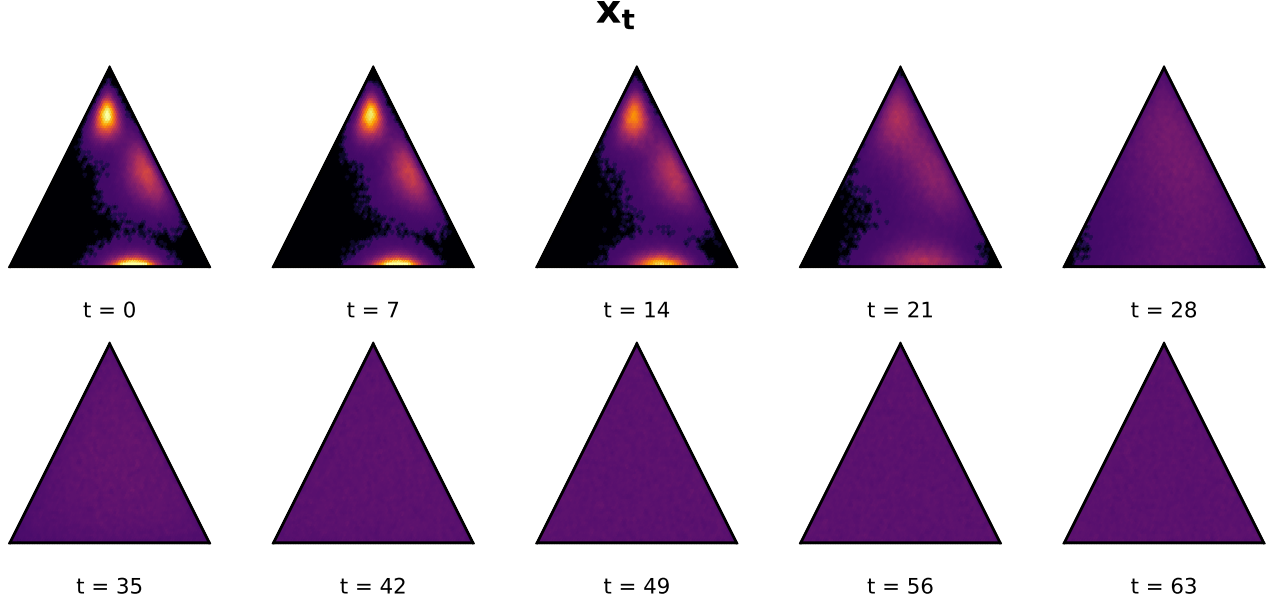


Figure 8: Visualization of the forward process in Dirichlet SS-DDPM on a three-dimensional probabilistic simplex.

## E.2. Beta

$$q(x_t|x_0) = \text{Beta}(x_t; \alpha_t, \beta_t) \quad (92)$$

There are many ways to define a noising schedule. We choose to fix the mode of the distribution at  $x_0$  and introduce a concentration parameter  $\nu_t$ , parameterizing  $\alpha_t = 1 + \nu_t x_0$  and  $\beta_t = 1 + \nu_t(1 - x_0)$ . By setting  $\nu_t$  to zero, we recover a uniform distribution, and by setting it to infinity we obtain a Dirac's delta, centered at  $x_0$ . Generally the Beta distribution has a two-dimensional sufficient statistic  $\mathcal{T}(x) = \begin{pmatrix} \log x \\ \log(1 - x) \end{pmatrix}$ . However, under this parameterization we can derive a one-dimensional tail statistic:

$$q(x_t|x_0) \propto \exp \{(\alpha_t - 1) \log x_t + (\beta_t - 1) \log(1 - x_t)\} = \exp \{\nu_t x_0 \log x_t + \nu_t(1 - x_0) \log(1 - x_t)\} = \quad (93)$$

$$= \exp \left\{ \nu_t x_0 \log \frac{x_t}{1 - x_t} + \nu_t \log(1 - x_t) \right\} = \exp \{ \eta_t(x_0) \mathcal{T}(x_t) + h_t(x_t) \} \quad (94)$$

Therefore we can use  $\eta_t(x_0) = \nu_t x_0$  and  $\mathcal{T}(x) = \log \frac{x}{1-x}$  to define the tail statistic:

$$\mathcal{G}_t(x_{t:T}) = \sum_{s=t}^T \nu_s \log \frac{x_s}{1 - x_s} \quad (95)$$

The KL divergence can then be calculated as follows:

$$D_{KL}(q^{ss}(x_t|x_0) \| p_\theta^{ss}(x_t|G_t)) = \log \frac{\text{Beta}(\alpha_t(x_\theta), \beta_t(x_\theta))}{\text{Beta}(\alpha_t(x_0), \beta_t(x_0))} + \nu_t(x_0 - x_\theta)(\psi(\alpha_t(x_0)) - \psi(\beta_t(x_0))) \quad (96)$$

## E.3. Dirichlet

$$q(x_t|x_0) = \text{Dirichlet}(x_t; \alpha_t^1, \dots, \alpha_t^K) \quad (97)$$

Similarly to the Beta distribution, we choose to fix the mode of the distribution at  $x_0$  and introduce a concentration parameter  $\nu_t$ , parameterizing  $\alpha_t^k = 1 + \nu_t x_0$ . This corresponds to using the natural parameter  $\eta_t(x_0) = \nu_t x_0$ . By setting  $\nu_t$  to zero,

we recover a uniform distribution, and by setting it to infinity we obtain a Dirac's delta, centered at  $x_0$ . We can use the sufficient statistic  $\mathcal{T}(x) = (\log x^1, \dots, \log x^{K^\top})$  to define the tail statistic:

$$\mathcal{G}_t(x_{t:T}) = \sum_{s=t}^T \nu_s (\log x_s^1, \dots, \log x_s^K)^\top \quad (98)$$

The KL divergence can then be calculated as follows:

$$D_{KL}(q^{ss}(x_t|x_0) \| p_\theta^{ss}(x_t|G_t)) = \sum_{k=1}^K \left[ \log \frac{\Gamma(\alpha_t^k(x_\theta))}{\Gamma(\alpha_t^k(x_0))} + \nu_t(x_0^k - x_\theta^k) \psi(\alpha_t^k(x_0)) \right] \quad (99)$$

#### E.4. Categorical

$$q(x_t|x_0) = \text{Cat}(x_t; p_t) \quad (100)$$

In this case we mimic the definition of categorical diffusion model, used in D3PM. The noising process is parameterized by the probability vector  $p_t = x_0 \bar{Q}_t$ . By setting  $\bar{Q}_0$  to identity, we recover a Dirac's delta, centered at  $x_0$ .

In this parameterization the natural parameter admits linearization (after some notation abuse):

$$\eta_t(x_0) = \log(x_0 \bar{Q}_t) = x_0 \log \bar{Q}_t, \text{ where} \quad (101)$$

$\log$  is taken element-wise, and we assume  $0 \log 0 = 0$ .

The sufficient statistic here is a vector  $x_t^\top$ . Therefore, the tail statistic can be defined as follows:

$$\mathcal{G}_t(x_{t:T}) = \sum_{s=t}^T (\log \bar{Q}_s \cdot x_s^\top) = \sum_{s=t}^T \log(\bar{Q}_s x_s^\top) \quad (102)$$

Note that, unlike in the Gaussian case, the categorical star-shaped diffusion is not equivalent to the categorical DDPM. The main difference here is that the input  $G_t$  to the predictive model  $x_\theta(G_t)$  is now a continuous vector instead of a one-hot vector.

#### E.5. von Mises

$$q(x_t|x_0) = \text{vonMises}(x_t; x_0, \kappa_t) \quad (103)$$

The von Mises distribution has two parameters, the mode  $x$  and the concentration parameter  $\kappa$ . It is natural to set the mode of the noising distribution to  $x_0$  and vary the concentration parameter  $\kappa_t$ . When  $\kappa_t$  goes to infinity, the von Mises distribution approaches a Dirac's delta, centered at  $x_0$ . When  $\kappa_t$  goes to 0, it approaches a uniform distribution on a unit circle. The sufficient statistic is  $\mathcal{T}(x_t) = \begin{pmatrix} \cos x_t \\ \sin x_t \end{pmatrix}$ , and the corresponding natural parameter is  $\eta_t(x_0) = \kappa_t$ . The tail statistic  $\mathcal{G}_t(x_{t:T})$  is therefore defined as follows:

$$\mathcal{G}_t(x_{t:T}) = \sum_{s=t}^T \kappa_s \begin{pmatrix} \cos x_s \\ \sin x_s \end{pmatrix} \quad (104)$$

The KL divergence term can be calculated as follows:

$$D_{KL}(q^{ss}(x_t|x_0) \| p_\theta^{ss}(x_t|G_t)) = \kappa_t \frac{I_1(\kappa_t)}{I_0(\kappa_t)} (1 - \cos(x_0 - x_\theta(G_t))) \quad (105)$$

#### E.6. von Mises–Fisher

$$q(x_t|x_0) = \text{vMF}(x_t; x_0, \kappa_t) \quad (106)$$

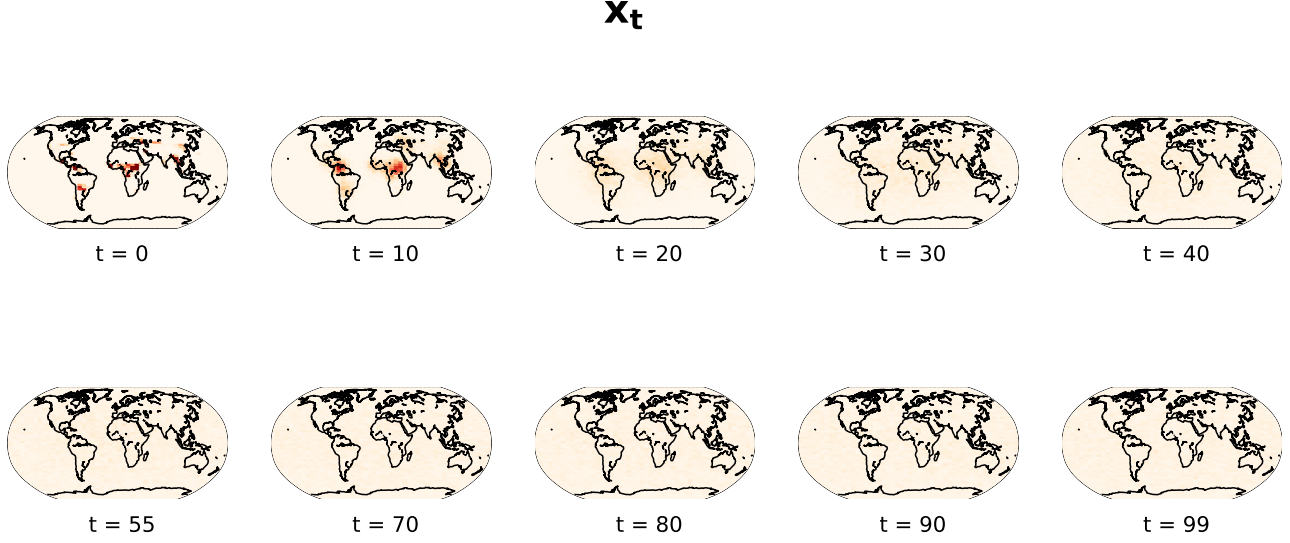


Figure 9: Visualization of the forward process in von Mises–Fisher SS-DDPM on a three-dimensional sphere.

Similar to the one-dimensional case, we set the mode of the distribution to  $x_0$ , and define the schedule using the concentration parameter  $\kappa_t$ . When  $\kappa_t$  goes to infinity, the von Mises–Fisher distribution approaches a Dirac’s delta, centered at  $x_0$ . When  $\kappa_t$  goes to 0, it approaches a uniform distribution on a unit sphere. The sufficient statistic is  $\mathcal{T}(x) = x$ , and the corresponding natural parameter is  $\eta_t(x_0) = \kappa_t$ . The tail statistic  $\mathcal{G}_t(x_{t:T})$  is therefore defined as follows:

$$\mathcal{G}_t(x_{t:T}) = \sum_{s=t}^T \kappa_s x_s \quad (107)$$

The KL divergence term can be calculated as follows:

$$D_{KL}(q^{ss}(x_t|x_0) \parallel p_\theta^{ss}(x_t|G_t)) = \kappa_t \frac{I_{K/2}(\kappa_t)}{I_{K/2-1}(\kappa_t)} x_0^\top (x_0 - x_\theta) \quad (108)$$

## E.7. Gamma

$$q(x_t|x_0) = \Gamma(x_t; \alpha_t, \beta_t) \quad (109)$$

There are many ways to define a schedule. We choose to interpolate the mean of the distribution from  $x_0$  at  $t = 0$  to 1 at  $t = T$ . This can be achieved with the following parameterization:

$$\beta_t(x_0) = \alpha_t(\xi_t + (1 - \xi_t)x_0^{-1}) \quad (110)$$

The mean of the distribution is  $\frac{\alpha_t}{\beta_t}$ , and the variance is  $\frac{\alpha_t}{\beta_t^2}$ . Therefore, we recover the Dirac’s delta, centered at  $x_0$ , when we set  $\xi_t$  to 0 and  $\alpha_t$  to infinity. To achieve some standard distribution that doesn’t depend in  $x_0$ , we can set  $\xi_t$  to 1 and  $\alpha_t$  to some fixed value  $\alpha_T$ .

In this parameterization the natural parameters are  $\alpha_t - 1$  and  $-\beta_t$ , and the corresponding sufficient statistics are  $\log x_t$  and  $x_t$ . Since the parameter  $\alpha_t$  doesn’t depend on  $x_0$ , we only need the sufficient statistic  $\mathcal{T}(x_t) = x_t$  to define the tail statistic:

$$\mathcal{G}(x_{t:T}) = \sum_{s=t}^T \alpha_s(1 - \xi_s)x_s \quad (111)$$

The KL divergence can be computed as follows:

$$D_{KL}(q^{ss}(x_t|x_0) \parallel p_\theta^{ss}(x_t|G_t)) = \alpha_t \left[ \log \frac{\beta_t(x_0)}{\beta_t(x_\theta(G_t, t))} + \frac{\beta_t(x_\theta(G_t, t))}{\beta_t(x_0)} - 1 \right] \quad (112)$$

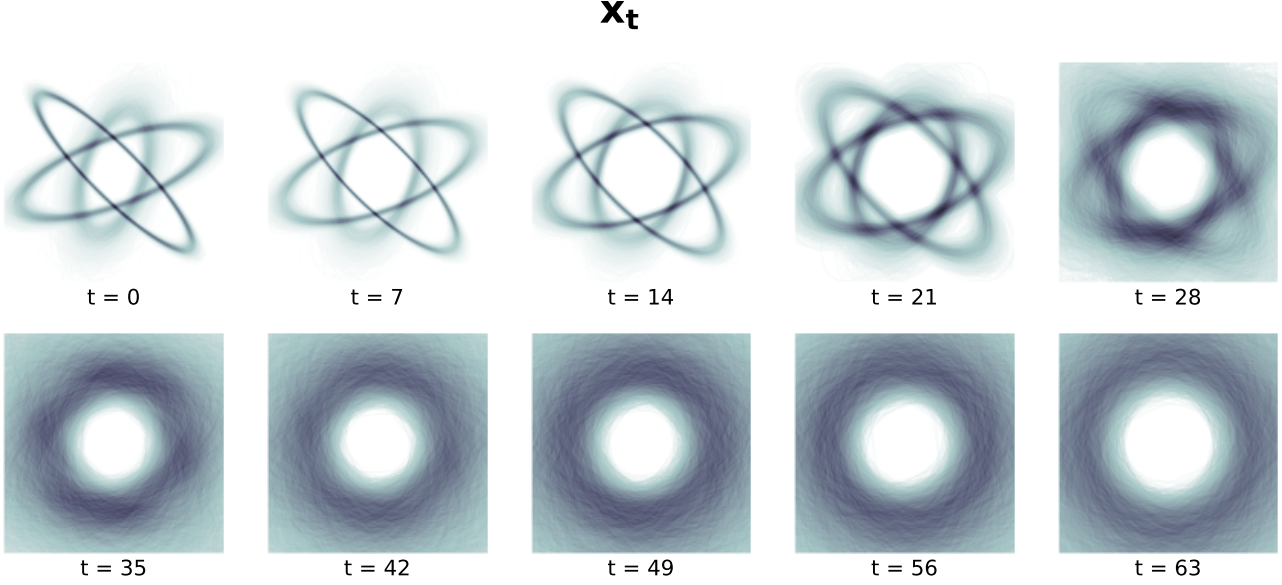


Figure 10: Visualization of the forward process in Wishart SS-DDPM on positive definite matrices of size  $2 \times 2$ .

### E.8. Wishart

$$q(X_t|X_0) = \mathcal{W}_p(X_t; V_t, n_t) \quad (113)$$

The natural parameters for the Wishart distribution are  $-\frac{1}{2}V_t^{-1}$  and  $\frac{n_t-p-1}{2}$ . To achieve linear parameterization, we need to linearly parameterize the inverse of  $V_t$  rather than  $V_t$  directly. Similar to the Gamma distribution, we interpolate the mean of the distribution from  $X_0$  at  $t = 0$  to  $I$  at  $t = T$ . This can be achieved with the following parameterization:

$$\mu_t(X_0) = \xi_t I + (1 - \xi_t)X_0^{-1} \quad (114)$$

$$V_t(X_0) = n_t^{-1}\mu_t^{-1}(X_0) \quad (115)$$

We recover the Dirac's delta, centered at  $X_0$ , when we set  $\xi_t$  to 0 and  $n_t$  to infinity. To achieve some standard distribution that doesn't depend in  $X_0$ , we set  $\xi_t$  to 1 and  $n_t$  to some fixed value  $n_T$ .

The sufficient statistic for this distribution is  $\mathcal{T}(X_t) = \begin{pmatrix} X_t \\ \log|X_t| \end{pmatrix}$ . Since the parameter  $n_t$  doesn't depend on  $X_0$ , we don't need the corresponding sufficient statistic  $\log|X_t|$ , and can use  $\mathcal{T}(X_t) = X_t$  to define the tail statistic:

$$\mathcal{G}(X_{t:T}, t) = \sum_{s=t}^T n_s(1 - \xi_s)X_t \quad (116)$$

The KL divergence can then be calculated as follows:

$$D_{KL}(q^{ss}(x_t|x_0) \| p_\theta^{ss}(x_t|G_t)) = -\frac{n_t}{2} [\log|V_t^{-1}(X_\theta)V_t(X_0)| - \text{tr}(V_t^{-1}(X_\theta)V_t(X_0)) + p] \quad (117)$$

### F. Choosing the noise schedule

In DDPMs we train a neural network to predict  $x_0$  given the current noisy sample  $x_t$ . In SS-DDPMs we use the tail statistic  $G_t$  as the neural network input instead. Therefore, it is natural to search for a schedule, where the “level of noise” in  $G_t$  is similar to the “level of noise” in  $x_t$  from some DDPM model. Similar to D3PM we formalize the “level of noise” as the mutual information between the clean and noisy samples. For SS-DDPM it would be  $I^{ss}(x_0; G_t)$ , and for DDPM it would be  $I^{DDPM}(x_0; x_t)$ . We would like to start from a well-performing DDPM model, and define a similar schedule by matching

$I^{\text{SS}}(x_0; G_t) \approx I^{\text{DDPM}}(x_0; x_t)$ . Since Gaussian SS-DDPM is equivalent to DDPM, the desired schedule can be found in Theorem 2. In general case, however, it is difficult to find a matching schedule.

In our experiments we found the following heuristic to work well enough. First, we find a Gaussian SS-DDPM schedule that is equivalent to the DDPM with the desired schedule. We denote the corresponding mutual information as  $I_{\mathcal{N}}^{\text{SS}}(x_0; G_t) = I^{\text{DDPM}}(x_0; x_t)$ . Then, we can match it in the original space of  $x_t$  and hope that the resulting mutual information in the space of tail statistics is close too:

$$I^{\text{SS}}(x_0; x_t) \approx I_{\mathcal{N}}^{\text{SS}}(x_0; x_t) \stackrel{?}{\Rightarrow} I^{\text{SS}}(x_0; G_t) \approx I_{\mathcal{N}}^{\text{SS}}(x_0; G_t) \quad (118)$$

Assuming the schedule is parameterized by a single parameter  $\nu$ , we can build a look-up table  $I^{\text{SS}}(x_0; x_\nu)$  for a range of parameters  $\nu$ . Then we can use binary search to build a schedule to match the mutual information  $I^{\text{SS}}(x_0; x_t)$  to the mutual information schedule  $I_{\mathcal{N}}^{\text{SS}}(x_0; x_t)$ . While this procedure doesn't allow to match the target schedule *exactly*, it provides a good enough approximation and allows to obtain an adequate schedule. We used this procedure to find the schedule for the Beta diffusion, used in Section 4.3.

To build the look-up table, we need a robust way to estimate the mutual information. The target mutual information  $I_{\mathcal{N}}^{\text{SS}}(x_0; x_t)$  can be computed analytically when the data  $q(x_0)$  follows a Gaussian distribution. When the data follows an arbitrary distribution, it can be approximated with a Gaussian mixture and the mutual information can be calculated using numerical integration. Estimating the mutual information for arbitrary noising distributions is more difficult. We find that the Kraskov estimator works well when the mutual information is high ( $I > 2$ ). When the mutual information is lower, we build a different estimator using DSIVI bounds (Molchanov et al., 2019).

$$I^{\text{SS}}(x_0; x_\nu) = D_{KL}(q^{\text{ss}}(x_0, x_t) \| q^{\text{ss}}(x_0)q^{\text{ss}}(x_t)) = \mathcal{H}[x_t] - \mathcal{H}[x_t|x_0] \quad (119)$$

This conditional entropy is available in closed form for many distributions in the exponential family. Since the marginal distribution  $q^{\text{ss}}(x_0, x_t) = \int q^{\text{ss}}(x_t|x_0)q(x_0)dx_0$  is a semi-implicit distribution (Yin & Zhou, 2018), we can use the DSIVI sandwich (Molchanov et al., 2019) to obtain an upper and lower bound on the marginal entropy  $\mathcal{H}[x_t]$ :

$$\mathcal{H}[x_t] = -\mathbb{E}_{q^{\text{ss}}} \log q^{\text{ss}}(x_t) = -\mathbb{E}_{q^{\text{ss}}} \log \int q^{\text{ss}}(x_t|x_0)q(x_0)dx_0 \quad (120)$$

$$\mathcal{H}[x_t] \geq -\mathbb{E}_{x_0^{0:K} \sim q(x_0)} \mathbb{E}_{x_t \sim q(x_t|x_0)|_{x_0=x_0^0}} \log \frac{1}{K+1} \sum_{k=0}^K q^{\text{ss}}(x_t|x_0^k) \quad (121)$$

$$\mathcal{H}[x_t] \leq -\mathbb{E}_{x_0^{0:K} \sim q(x_0)} \mathbb{E}_{x_t \sim q(x_t|x_0)|_{x_0=x_0^0}} \log \frac{1}{K} \sum_{k=1}^K q^{\text{ss}}(x_t|x_0^k) \quad (122)$$

These bounds are asymptotically exact and can be estimated using Monte-Carlo. We use  $K = 1000$  when the mutual information is high ( $\frac{1}{2} \leq I < 2$ ),  $K = 100$  when the mutual information is lower ( $0.002 \leq I < \frac{1}{2}$ ), and estimate the expectations using  $M = 10^8 K^{-1}$  samples for each timestamp. For values  $I > 2$  we use the Kraskov estimator with  $M = 10^5$  samples and  $k = 10$  neighbors. For values  $I < 0.002$  we fit an exponential curve  $i(t) = e^{at+b}$  to interpolate between the noisy SIVI estimates, obtained with  $K = 50$  and  $M = 10^5$ .

For evaluating the mutual information  $I(x_0; G_t)$  between the clean data and the tail statistics, we use the Kraskov estimator with  $k = 10$  and  $M = 10^5$ .

The mutual information look-up table for the Beta star-shaped diffusion, as well as the used estimations of the mutual information, are presented in Figure 11. The resulting schedule for the beta diffusion is presented in Figure 12, and the comparison of the mutual information schedules for the tail statistics between Beta SS-DDPM and the referenced Gaussian SS-DDPM is presented in Figure 13.

## G. Normalizing the tail statistics

We illustrate different strategies of normalizing the tail statistics in Figure 14. Normalizing by the sum of coefficients is not enough, therefore we resort to matching the mean and the variance empirically.

Also, proper normalization can allow us to visualize the tail statistics by projecting them back into the original domain using  $\mathcal{T}^{-1}(\tilde{G}_t)$ . The effect of normalization is illustrated in Figure 15.

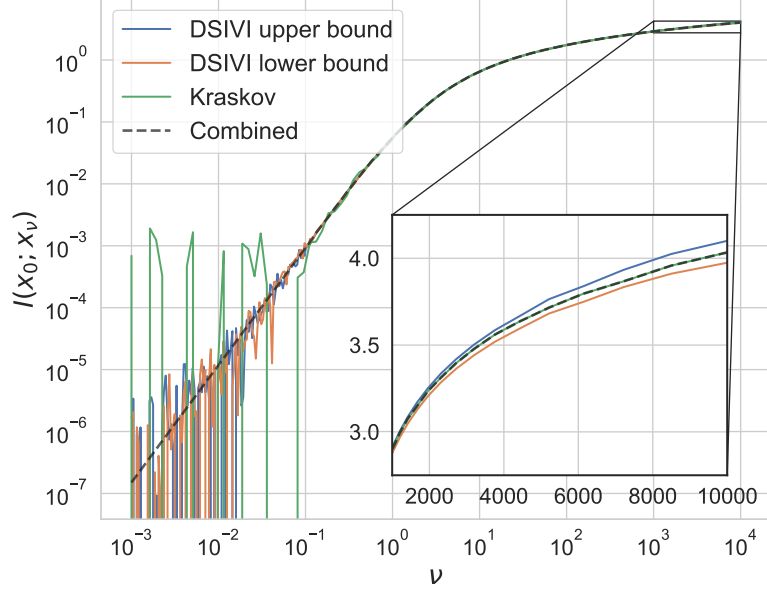


Figure 11: The mutual information look-up table for Beta star-shaped diffusion.

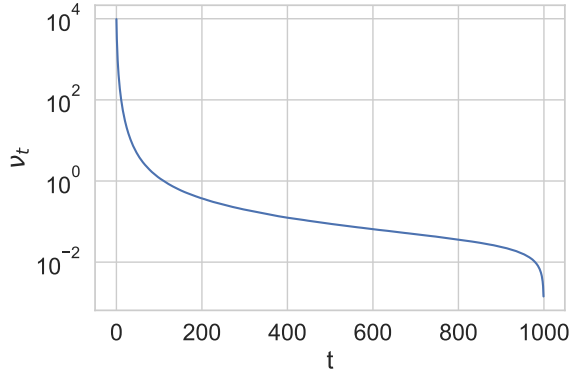


Figure 12: The schedule for Beta star-shaped diffusion.

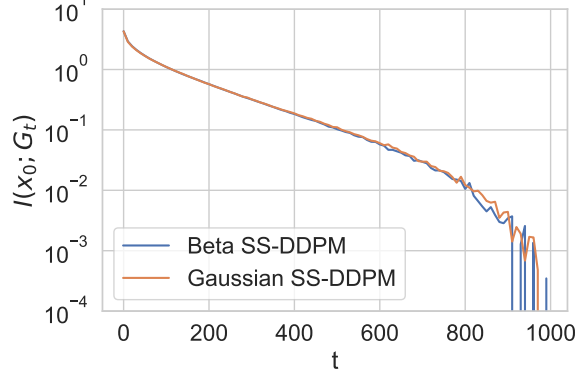


Figure 13: Mutual information between clean data and the tail statistics for beta star-shaped diffusion.

## H. Changing discretization

When sampling from DDPMs, we can skip some timestamps to trade off computations for quality of the generated samples. For example, we can generate  $x_{t_1}$  from  $x_{t_2}$  in one step, without generating the intermediate variables  $x_{t_1+1:t_2-1}$ :

$$\tilde{p}_\theta^{\text{DDPM}}(x_{t_1} | x_{t_2}) = q^{\text{DDPM}}(x_{t_1} | x_{t_2}, x_0) |_{x_0=x_\theta^{\text{DDPM}}(x_{t_2}, t_2)} = \quad (123)$$

$$= \mathcal{N} \left( x_{t_1}; \frac{\sqrt{\bar{\alpha}_{t_1}^{\text{DDPM}}} \left( 1 - \frac{\bar{\alpha}_{t_2}^{\text{DDPM}}}{\bar{\alpha}_{t_1}^{\text{DDPM}}} \right) x_\theta^{\text{DDPM}}(x_{t_2}, t_2) + \frac{\sqrt{\bar{\alpha}_{t_2}^{\text{DDPM}}} (1 - \bar{\alpha}_{t_1}^{\text{DDPM}})}{1 - \bar{\alpha}_{t_2}^{\text{DDPM}}} x_{t_2}, \frac{1 - \bar{\alpha}_{t_1}^{\text{DDPM}}}{1 - \bar{\alpha}_{t_2}^{\text{DDPM}}} \left( 1 - \frac{\bar{\alpha}_{t_2}^{\text{DDPM}}}{\bar{\alpha}_{t_1}^{\text{DDPM}}} \right)} \right) = \quad (124)$$

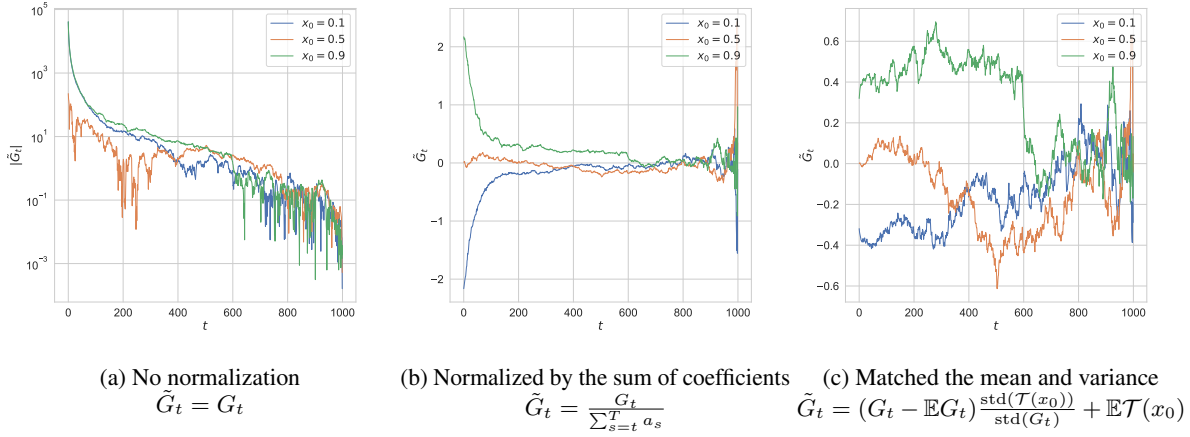


Figure 14: Example trajectories of the normalized tail statistics with different normalization strategies. The trajectories are coming from a single dimension of Beta SS-DDPM.

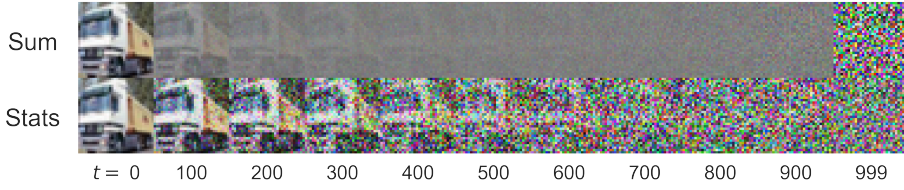


Figure 15: Visualizing the tail statistics for Beta SS-DDPM with different normalization by mapping the normalized tail statistics  $\tilde{G}_t$  into the data domain using  $\mathcal{T}^{-1}(\tilde{G}_t)$ . Top row: normalized by the sum of coefficients,  $\tilde{G}_t = \frac{G_t}{\sum_{s=t}^T a_s}$ . Bottom row: matched the mean and variance,  $\tilde{G}_t = (G_t - \mathbb{E}G_t) \frac{\text{std}(\mathcal{T}(x_0))}{\text{std}(G_t)} + \mathbb{E}\mathcal{T}(x_0)$

$$= \mathcal{N} \left( x_{t_1}; \frac{\bar{\alpha}_{t_1}^{\text{DDPM}} - \bar{\alpha}_{t_2}^{\text{DDPM}}}{\sqrt{\bar{\alpha}_{t_1}^{\text{DDPM}}(1 - \bar{\alpha}_{t_2}^{\text{DDPM}})}} x_{\theta}^{\text{DDPM}}(x_{t_2}, t_2) + \frac{\sqrt{\bar{\alpha}_{t_2}^{\text{DDPM}}(1 - \bar{\alpha}_{t_1}^{\text{DDPM}})}}{\sqrt{\bar{\alpha}_{t_1}^{\text{DDPM}}(1 - \bar{\alpha}_{t_2}^{\text{DDPM}})}} x_{t_2}, \frac{(1 - \bar{\alpha}_{t_1}^{\text{DDPM}})(\bar{\alpha}_{t_1}^{\text{DDPM}} - \bar{\alpha}_{t_2}^{\text{DDPM}})}{(1 - \bar{\alpha}_{t_2}^{\text{DDPM}})\bar{\alpha}_{t_1}^{\text{DDPM}}} \right) \quad (125)$$

In the general case of SS-DDPM, we can't just skip the variables. If we skip the variables, the corresponding tail statistics will become atypical and the generative process will fail. To keep the tail statistics adequate, we can sample all the intermediate variables  $x_t$ , but do it in a way that doesn't use additional function evaluations:

$$G_{t_1} = \sum_{s=t_1}^{t_2-1} A_s^{\top} \mathcal{T}(x_s) + G_{t_2}, \text{ where} \quad (126)$$

$$x_s \sim q(x_s | x_0) \Big|_{x_0=x_{\theta}^{\text{SS}}(G_{t_2}, t_2)} \quad (127)$$

In case of Gaussian SS-DDPM this trick is equivalent to skipping the variables in DDPM:

$$G_{t_1} = \frac{1 - \bar{\alpha}_{t_1}^{\text{DDPM}}}{\sqrt{\bar{\alpha}_{t_1}^{\text{DDPM}}}} \sum_{s=t_1}^{t_2-1} \frac{\sqrt{\bar{\alpha}_s^{\text{SS}}} x_s}{1 - \bar{\alpha}_s^{\text{SS}}} + \frac{1 - \bar{\alpha}_{t_1}^{\text{DDPM}}}{\sqrt{\bar{\alpha}_{t_1}^{\text{DDPM}}}} \frac{\sqrt{\bar{\alpha}_{t_2}^{\text{DDPM}}}}{1 - \bar{\alpha}_{t_2}^{\text{DDPM}}} G_{t_2} = \quad (128)$$

$$= \frac{1 - \bar{\alpha}_{t_1}^{\text{DDPM}}}{\sqrt{\bar{\alpha}_{t_1}^{\text{DDPM}}}} \sum_{s=t_1}^{t_2-1} \frac{\bar{\alpha}_s^{\text{SS}}}{1 - \bar{\alpha}_s^{\text{SS}}} x_{\theta}^{\text{SS}}(G_{t_2}, t_2) + \frac{1 - \bar{\alpha}_{t_1}^{\text{DDPM}}}{\sqrt{\bar{\alpha}_{t_1}^{\text{DDPM}}}} \sum_{s=t_1}^{t_2-1} \sqrt{\frac{\bar{\alpha}_s^{\text{SS}}}{1 - \bar{\alpha}_s^{\text{SS}}}} \epsilon_s + \frac{\sqrt{\bar{\alpha}_{t_2}^{\text{DDPM}}(1 - \bar{\alpha}_{t_1}^{\text{DDPM}})}}{\sqrt{\bar{\alpha}_{t_1}^{\text{DDPM}}(1 - \bar{\alpha}_{t_2}^{\text{DDPM}})}} G_{t_2} \quad (129)$$

$$\mathbb{E}G_{t_1} = \frac{1 - \bar{\alpha}_{t_1}^{\text{DDPM}}}{\sqrt{\bar{\alpha}_{t_1}^{\text{DDPM}}}} \left( \frac{\bar{\alpha}_{t_1}^{\text{DDPM}}}{1 - \bar{\alpha}_{t_1}^{\text{DDPM}}} - \frac{\bar{\alpha}_{t_2}^{\text{DDPM}}}{1 - \bar{\alpha}_{t_2}^{\text{DDPM}}} \right) x_{\theta}^{\text{SS}}(G_{t_2}, t_2) + \frac{\sqrt{\bar{\alpha}_{t_2}^{\text{DDPM}}(1 - \bar{\alpha}_{t_1}^{\text{DDPM}})}}{\sqrt{\bar{\alpha}_{t_1}^{\text{DDPM}}(1 - \bar{\alpha}_{t_2}^{\text{DDPM}})}} G_{t_2} = \quad (130)$$

$$= \frac{(1 - \bar{\alpha}_{t_1}^{\text{DDPM}})(\bar{\alpha}_{t_1}^{\text{DDPM}} - \bar{\alpha}_{t_2})}{\sqrt{\bar{\alpha}_{t_1}^{\text{DDPM}}(1 - \bar{\alpha}_{t_1}^{\text{DDPM}})(1 - \bar{\alpha}_{t_2}^{\text{DDPM}})}} x_{\theta}^{\text{ss}}(G_{t_2}, t_2) + \frac{\sqrt{\bar{\alpha}_{t_2}^{\text{DDPM}}(1 - \bar{\alpha}_{t_1}^{\text{DDPM}})}}{\sqrt{\bar{\alpha}_{t_1}^{\text{DDPM}}(1 - \bar{\alpha}_{t_2}^{\text{DDPM}})}} G_{t_2} = \quad (131)$$

$$= \frac{(\bar{\alpha}_{t_1}^{\text{DDPM}} - \bar{\alpha}_{t_2})}{\sqrt{\bar{\alpha}_{t_1}^{\text{DDPM}}(1 - \bar{\alpha}_{t_2}^{\text{DDPM}})}} x_{\theta}^{\text{ss}}(G_{t_2}, t_2) + \frac{\sqrt{\bar{\alpha}_{t_2}^{\text{DDPM}}(1 - \bar{\alpha}_{t_1}^{\text{DDPM}})}}{\sqrt{\bar{\alpha}_{t_1}^{\text{DDPM}}(1 - \bar{\alpha}_{t_2}^{\text{DDPM}})}} G_{t_2} \quad (132)$$

$$\mathbb{D}G_{t_1} = \frac{(1 - \bar{\alpha}_{t_1}^{\text{DDPM}})^2}{\bar{\alpha}_{t_1}^{\text{DDPM}}} \sum_{s=t_1}^{t_2-1} \frac{\bar{\alpha}_s^{\text{ss}}}{1 - \bar{\alpha}_s^{\text{ss}}} = \frac{(1 - \bar{\alpha}_{t_1}^{\text{DDPM}})^2}{\bar{\alpha}_{t_1}^{\text{DDPM}}} \frac{\bar{\alpha}_{t_1}^{\text{DDPM}} - \bar{\alpha}_{t_2}^{\text{DDPM}}}{(1 - \bar{\alpha}_{t_1}^{\text{DDPM}})(1 - \bar{\alpha}_{t_2}^{\text{DDPM}})} = \quad (133)$$

$$= \frac{(1 - \bar{\alpha}_{t_1}^{\text{DDPM}})(\bar{\alpha}_{t_1}^{\text{DDPM}} - \bar{\alpha}_{t_2}^{\text{DDPM}})}{(1 - \bar{\alpha}_{t_2}^{\text{DDPM}})\bar{\alpha}_{t_1}^{\text{DDPM}}} \quad (134)$$

In general case this trick can be formalized as the following approximation to the reverse process:

$$p_{\theta}^{\text{ss}}(x_{t_1:t_2}|G_{t_2}) = \prod_{t=t_1}^{t_2} q^{\text{ss}}(x_t|x_0)|_{x_0=x_{\theta}(\mathcal{G}_t(x_{t:T}), t)} \approx \prod_{t=t_1}^{t_2} q^{\text{ss}}(x_t|x_0)|_{x_0=x_{\theta}(\mathcal{G}_{t_2}(x_{t_2:T}), t_2)} \quad (135)$$

Table 2: Examples of SS-DDPM in different families. There are many different ways to parameterize the distributions and the corresponding schedules. Further details are discussed in Appendix E.1–E.8.

DISTRIBUTION $q^{\text{ss}}(x_t x_0)$	NOISING SCHEDULE	TAIL STATISTIC $\mathcal{G}_t(x_{t:T})$	KL DIVERGENCE $D_{KL}(q^{\text{ss}}(x_t x_0) \parallel p_{\theta}^{\text{ss}}(x_t x_{t+1:T}))$
GAUSSIAN $N(x_t; \sqrt{\bar{\alpha}_t}x_0, 1 - \bar{\alpha}_t)$ $x_t \in \mathbb{R}$	$1 \xleftarrow[t \rightarrow 0]{} \bar{\alpha}_t \xrightarrow[t \rightarrow T]{} 0$	$\frac{1 - \bar{\alpha}'_s}{\sqrt{\bar{\alpha}'_s}} \sum_{s=t}^T \frac{\sqrt{\bar{\alpha}_s} x_s}{1 - \bar{\alpha}_s},$ where $\bar{\alpha}'_t = \frac{\sum_{s=t}^T \frac{\bar{\alpha}_s}{1 - \bar{\alpha}_s}}{1 + \sum_{s=t}^T \frac{\bar{\alpha}_s}{1 - \bar{\alpha}_s}}$	$\frac{\bar{\alpha}_t(x_\theta - x_0)^2}{2(1 - \bar{\alpha}_t)}$
BETA $\text{Beta}(x_t; \alpha_t(x_0), \beta_t(x_0))$ $x_t \in [0, 1]$	$\alpha_t(x_0) = 1 + \nu_t x_0$ $\beta_t(x_0) = 1 + \nu_t(1 - x_0)$ $+\infty \xleftarrow[t \rightarrow 0]{} \nu_t \xrightarrow[t \rightarrow T]{} 0$	$\sum_{s=t}^T \nu_s \log \frac{x_s}{1 - x_s}$	$\log \frac{\text{Beta}(\alpha_t(x_\theta), \beta_t(x_\theta))}{\text{Beta}(\alpha_t(x_0), \beta_t(x_0))} +$ $+ \nu_t(x_0 - x_\theta)(\psi(\alpha_t(x_0)) - \psi(\beta_t(x_0)))$
DIRICHLET $\text{Dir}(x_t; \alpha_1^1(x_0), \dots, \alpha_K^1(x_0))$ $x_t \in [0, 1]^K$ $\sum_{i=1}^K x_t^i = 1$	$\alpha_t^k(x_0) = 1 + \nu_t x_0^k$ $+\infty \xleftarrow[t \rightarrow 0]{} \nu_t \xrightarrow[t \rightarrow T]{} 0$	$\sum_{s=t}^T \nu_s \log x_s$	$\sum_{k=1}^K \left[ \log \frac{\Gamma(\alpha_t^k(x_\theta))}{\Gamma(\alpha_t^k(x_0))} + \right. \right. \left. \left. + \nu_t(x_0^k - x_\theta^k) \psi(\alpha_t^k(x_0)) \right] \right]$
CATEGORICAL $\text{Cat}(x_t; p_t(x_0))$ $x_t \in \{0, 1\}^D$ $\sum_{i=1}^D x_t^i = 1$	$p_t(x_0) = x_0 \bar{Q}_t$ $I \xleftarrow[t \rightarrow 0]{} \bar{Q}_t \xrightarrow[t \rightarrow T]{} \bar{Q}_T$	$\sum_{s=t}^T \log (\bar{Q}_s x_s^T)$	$\sum_{i=1}^D (p_t(x_0))_i \log \frac{(p_t(x_0))_i}{(p_t(x_\theta))_i}$
VON MISES $\text{vM}(x_t; x_0, \kappa_t)$ $x_t \in [-\pi, \pi]$	$+\infty \xleftarrow[t \rightarrow 0]{} \kappa_t \xrightarrow[t \rightarrow T]{} 0$	$\sum_{s=t}^T \kappa_s \begin{pmatrix} \cos x_s \\ \sin x_s \end{pmatrix}$	$\kappa_t \frac{I_1(\kappa_t)}{I_0(\kappa_t)} (1 - \cos(x_0 - x_\theta))$
VON MISES–FISHER $\text{vMF}(x_t; x_0, \kappa_t)$ $x_t \in [-1, 1]^K$ $\ x_t\  = 1$	$+\infty \xleftarrow[t \rightarrow 0]{} \kappa_t \xrightarrow[t \rightarrow T]{} 0$	$\sum_{s=t}^T \kappa_s x_s$	$\kappa_t \frac{I_{K/2}(\kappa_t)}{I_{K/2-1}(\kappa_t)} x_0^T (x_0 - x_\theta)$
GAMMA $\Gamma(x_t; \alpha_t, \beta_t(x_0))$ $x_t \in (0, +\infty)$	$\beta_t(x_0) = \alpha_t(\xi_t + (1 - \xi_t)x_0^{-1})$ $+\infty \xleftarrow[t \rightarrow 0]{} \alpha_t \xrightarrow[t \rightarrow T]{} \alpha_T$ $0 \xleftarrow[t \rightarrow 0]{} \xi_t \xrightarrow[t \rightarrow T]{} 1$	$\sum_{s=t}^T \alpha_s(1 - \xi_s)x_s$	$\alpha_t \left[ \log \frac{\beta_t(x_0)}{\beta_t(x_\theta(G_t, t))} + \right. \right. \left. \left. + \frac{\beta_t(x_\theta(G_t, t))}{\beta_t(x_0)} - 1 \right] \right]$
WISHART $\mathcal{W}(X_t; n_t, V_t(X_0))$ $X_t \in \mathbb{R}^{p \times p}$ $X_t \succ 0$	$\mu_t(X_0) = \xi_t I + (1 - \xi_t)X_0^{-1}$ $V_t(X_0) = n_t^{-1} \mu_t^{-1}(X_0)$ $+\infty \xleftarrow[t \rightarrow 0]{} n_t \xrightarrow[t \rightarrow T]{} n_T$ $0 \xleftarrow[t \rightarrow 0]{} \xi_t \xrightarrow[t \rightarrow T]{} 1$	$\sum_{s=t}^T n_s(1 - \xi_s)X_s$	$-\frac{n_t}{2} [\log  V_t^{-1}(X_\theta)V_t(X_0)  -$ $- \text{tr}(V_t^{-1}(X_\theta)V_t(X_0)) + p]$